Statistical Mechanics and Dynamics of the Outer Solar System. II. The Saturn/Uranus and Uranus/Neptune Zones.

KEVIN R. GRAZIER[1,2], WILLIAM 1. NEWMAN[1,3], WILLIAM M. KAULA[1,4], and JAMES M. HYMAN[5]

Abstract:

We report on numerical simulations exploring the dynamical stability of planetesimals in the gaps between the outer solar system planets. We reconsider the existence of stable niches in the Saturn/Uranus and Uranus/Neptune zones by employing 10,000 massless particles-many more than previous studies in these two zones---- using high-order optimized multi-step integration schemes coupled with roundoff error minimizing methods. An additional feature of this study, differing from its predecessors, is the fact that our initial distributions contain particles on orbits which are both inclined and non-circular. These initial distributions were also gaussian distributed such that the gaussian peaks were at the midpoint between the neighboring perturbers. The simulations showed an initial transient phase where the bulk of the primordial planetesimal swarm was removed from the solar system within 105 years. This is about 10 times longer than we observed in our previous Jupiter/Saturn studies. Next, there was a gravitational relaxation phase where the particles underwent a random walk in momentum space, and were exponentially eliminated by random encounters with the planets. Unlike our previous Jupiter/Saturn simulation, the particles did not fully relax into a third Lagrangian niche phase where long-lived particles are at Lagrange points or stable niches. 'I'his is either because the Lagrangian niche phase never occurs, or because these simulations did not have enough particles for this third phase to manifest. In these simulations, there was a general trend for the particles to migrate outward, and eventually

1. Department of Earth and Space Sciences, University of California, Los Angeles. CA 9009.5.
2. Jet Propulsion Laboratory. California Institute of Technology, Pasadena, CA, 91109.
3. Departments of Physics and Astronomy, and Mathematics. University of California, Los Angeles, CA 9009.5.
4. Institute of Geophysics and Planetary Physics. [University of California, Los Angeles. CA 90095.
.5. Theoretical Division, Los Alamos National Laboratory, Los Alamos, NM 87545.

to be cleared out by the outermost planet, in thezone. We confirmed that particles with higher eccentricities had shorter lifetimes. and that the resonances between the Jovian planets "pumped up" the eccentricities of the planetesimals with low-inclination orbits more than those with higher inclinations. This resulted in longer lifetimes for the particles with a large initial inclination. We estimated the expected lifetime of particles using kinetic theory and even though the time scale of the Uranus/Neptune simulation was 380 times longer than our previous Jupiter/Saturn simulation, the planetesimals in the Uranus/ Nept une zone were cleared out more quickly than those in the Saturn/Uranus zone because of the positions of resonances with the Jovian planets. These resonances had an even greater effect than random gravitational stirring in the winnowing process and confirm that all the Jovian planets are necessary in long simulations. Even though we observed several long lived zones at 12.5, 14.4, 16, 24..5 and 26 AU, only two particles remained at the end of the 10^9 year integration: one near the 2:3 Saturn resonance, and the other near the Neptune 1:1 resonance. This suggests that niches for planetesimal material in the Jovian planets are rare and may exist either only in extremely narrow bands, or in the neighborhoods of the triangular Lagrange points of the outer planets.

1. INTRODUCTION

Why is there an apparent lack of planetesimal material between the outer planets in the solar system? Is it due to observational bias—the bodies are there, but are distant and dark and just can not be observed? Did these regions suffer an *ab initio* depletion of planetesimal material for reasons as-of-yet not understood? Or is it simply that these regions are dynamically unstable over long time periods? This third hypothesis is one we can test. We therefore seek to explore the dynamical stability of planetesimals in the gaps between the outer solar system planets by simulating the evolution of 10,000 massless test particles places in each of the interplanet gaps. The particles are initially on random orbits (selected from the prescription described below), and

their trajectories simulated using high-order optimized multi-step integration schemes coupled with roundoff error minimizing methods.

In contrast with the Jupiter/Saturn zone, there have been comparatively few computational studies of planetesimal lifetimes in the Saturn/Uranus and Uranus/Neptune zones. This is almost certainly a byproduct of the extreme computational expense that results from the much slower dynamical evolution of these regions when compared to the Jupiter/Saturn zone. Indeed, our present studies—with ten times fewer particles than our Jupiter/Saturn simulation (Grazier et al., 1997, hereafter called Paper I)—took approximately 30 times as many CPU hours. (Using the kinetic theory we derived in Paper I to estimate depletion rates, our *ab initio* calculations predicted that the initial rate of depletion of planetesimals would be a factor 80 slower than in the Jupiter/Saturn case, growing to a factor of at least 200. In the simulations, the second number was more nearly 400.) In the early stages of this simulation, we employed as many as 50 fast Hewlett-Packard workstations running simultaneously, each having identical planetary positions, but with different planetesimal populations selected to focus attention on the zones of particular interest.

Observationally, there are very few objects known to have orbits whose semimajor axes lie in the range between Saturn and Neptune. The Jet Propulsion Laboratory maintains the *Horizons* database of all known solar system bodies for which the orbits are well-determined (Giorgini, et al. 1996). This database contains only eight asteroids, known as Centaurs. whose semimajor axes lie in the Saturn/Uranus or Uranus/Neptune zones. Even the term '-asteroid'" can be nebulous in describing bodies in the outer solar system. because the composition of many such bodies are more cometary in nature. Chiron, probably the most well-known Centaur. has both an asteroid designation (2060 Chiron), and a comet designation (95P/Chiron). The latter was a result of the observations that Chiron has both a dust coma (Meech and Belton, 1989), and exhibits bursts

Nine percent of their initial sample survived the entire simulation, however.

In 1989, Duncan. Quinn, and Tremaine (hereafter referred to as DQT89) defined a two-adjacent-planet mapping that approximated the restricted three-body problem. In their model. planets were confined to circular, coplanar orbits: test particles had initially small eccentricities and were similarly confined to the invariable plane. Particle orbits were treated as Keplerian, except at conjunctions where they were given impulsive perturbations. Using this mapping method, they examined the zones between each of the outer planets for up to 4..5 Gy. They found that many of the nearly circular orbits in both the Saturn/Uranus and Uranus/Neptune gaps might survive over the lifetime of the solar system—in what they called "Kuiper Bands. "

The following year, Gladman and Duncan (1990; hereafter GD90), presented results that were in dramatic contrast with DQT89. Using a fourth-order symplectic mapping method developed by Candy and Rozmus (1990), GD90 performed a three-dimensional integration of the trajectories of 180 nearly circular. coplanar zero-inclination particles—90 in each of the Saturn/Uranus and Uranus/Neptune zones—for up to 22.5 My. The positions and velocities of the planets in their 'simulation were not coplanar and were selected according to the LONGSTOP1B initial conditions (Nobili et al., 1989). They found that most of the test particles were removed by close approaches within 10 My. GD90 reported that one band, centered at about 26 AU, contained particles that survived the entire integration while maintaining low eccentricities. They concluded that the survival of this band over solar system lifetimes was doubtful.

Holman and Wisdom (1993; hereafter HW93) used their symplectic mapping technique (Wisdom and Holman, 1991) to survey the outer solar system for stable orbits in the range from 5 to .50 AU. In the HW93 simulations. the integrations were performed in three-dimensions-using three-dimensional initial planetary conditions from Cohen. Hubbard and Oesterwinter (1973)—but with all planetesimals initially on zero-inclination circular orbits. After an 800 My simulation. they

found that uo particles survived between Saturn and Uranus, and only six (out of 438) survived between Uranus and Neptune. Similar to GD90, four of these were near 26 AU. HW93, like GD90, found that most of the test particles in these zones were removed on 10^7-year timescales. HW93 also performed integrations of particles initially situated at the triangular Lagrange points of the outer three planets. They found that the neighborhood near the L4 and L5 points of Uranus and Neptune were stable for up to 20 My. The corresponding points for Saturn were unstable. though particles initially situated in an annular region surrounding the L4 ancl L5 points were stable for 20 My time frames. This last result was corroborated by de la Barre et al., (1996) who found Saturn librators (which they termed "Bruins"), which were stable for up to 412 My.

Levison and Duncan (1993) and Duncan and Quinn (1993) reported the results of a study where they used a modified Wisdom- Holman scheme, in which the planetary motions were determined from a synthetic secular perturbation theory, to examine these regions for up to 1 Gy. Using low-inclination, nearly circular orbits, they found that nearly all of the test particles initially in these zones became planet-crossers wit hin 10^8 years—except for a few long-lived bands at 16, 24, and, again, 26 AU. All particles became planet-crossing by 10^9 years. We now turn our attention to the computational methods used in our simulation.

3. NUMERICAL METHOD AND INITIALIZATION

The numerical method used for the integration is a roundoff-minirnized truncation-controlled 13th order modified Störmer method (Newman et al.. 1990; Newman et al.. 1993; Bell et al., 1994; Newman et al., 199.5, 1997). We expanded upon this methodology in Paper I. and presented the results of several tests designed to determine the energy and longitude error growth properties of this integration method. Adding the mass of the terrestrial planets to that of the sun. we performed several integrations of the Jovian planets. For sixteen different sets of initial conditions generated from the DE245 ephemeris (Standish. personal communication. 1994). we integrated the

trajectories of the Jovian planets for a time interval equivalent to 2^n Jupiter orbits. where n is an integer between O and 20. At the end of each integration. we use the positions and velocities of the Sun and planets as starting conditions to integrate *backwards* in time. In the absence of systematic integration error (i.e., if the error growth is controlled by roundoff error as opposed to truncation error), we should see energy error grow as $t^{1/2}$; angular position errors should grow as $t^{3/2}$. Figure 1 is reprinted from Paper I, and shows the relative RMS energy error for the entire system. We can see that the energy error grows as $t^{0.46}$, very nearly $t^{1/2}$, indicating the absence of systematic error growth.

Figure 2 shows the RMS angular position errors for all of the Jovian planets. Given initial position for a planet as $\vec{r}_i$, and final position $\vec{r}_f$, wc define the angular position error λ as:

$$\lambda = \arcsin\left(\frac{|\vec{r}_i \times \vec{r}_f|}{|\vec{r}_i||\vec{r}_f|}\right) \quad .$$

The angular position errors of all the Jovian planets grow at rates less than $t^{3/2}$ and after 2^{21} Jupiter orbits (nearly 25 million years), the errors for all planets are less than of 2 x 10^{-5} radians. Extrapolated, the angular position error after 10^9 years is less than a degree for all planets!

Our simulation began with ten thousand test particles placed in elliptical, inclined heliocentric orbits, and their trajectories were integrated for up to 1 billion years—or until they were removed from the simulation. The sun and all of the Jovian planets were included as perturbers and were mutually interacting. but the test particles were treated as massless. Initial planetary positions were determined for one epoch from the DE245 ephemeris (Standish. personal communication, 1994) and were identical to those in our Jupiter/Saturn study. Although input/output was given in heliocentric coordinates, all integrations were performed in a barycentric frame.

The initial test particle sernimajor axes were C;aussian-distributed so that the mean semimajor axis peaked at the mean value of the two neighboring planets (14.35 AU for Saturn/Uranus: 24.62

for Uranus/Neptune), and the 3σ points were coincident with the planets' orbits. No orbits were allowed within 0..5 AU of the innermost planet or 0.5 AU beyond the outermost,. The initial inclinations were similarly Gaussian-distributed with a mean of 0° and a standard deviation of 10°. Eccentricities were randomly chosen from O to 1 from an exponential distribution with an e-folding constant of 0.1. The initial phase angles, longitudes of nodes, and longitudes of perihelia were randomly selected from a uniform distribution between O and 2π. Random number generation was performed using procedures RAN2, EXPDEV and GASDEV from Press et al. (1988).

In this simulation, a test particle was considered to be eliminated if it met one of three criteria—exactly those we used for Jupiter/Saturn. Particles were removed from the simulation if they underwent a close-encounter and passed within the activity sphere of a planet. Here, we used the modified definition of activity radius (Holman and Wisdom, 1993; Danby, 1988) namely

$$r_{act} = a_0 \left(\frac{m_p}{M_\odot} \right)^{2/5} ,$$

where m_p is the mass of a given planet, and a. is its initial semimajor axis. A particle was considered ejected from the solar system, and thus removed from the simulation, if (1) it had 'positive energy relative to the Sun and all of the planets, (2) it had heliocentric radius greater than 50.0 AU, and (3) the projection of its velocity against a radial line from the Sun was positive, i.e., was on an outbound trajectory with $\vec{r} \cdot \vec{v} > 0$. Finally, if a particle came within 1 AU of the Sun, we calculated its perihelion distance. If this was less than the radius of the solar photosphere. then we eliminated the particle from the simulation. Similar to our Jupiter/Saturn study. no such "Sun-grazers" were detected for either Saturn/Uranus or Uranus/Neptune planetesimals.

4. RESULTS

'The Saturn/Uranus Zone.

In our Jupiter/Saturn study. we delineated three distinct phases in the evolution of particles situated in the interplanet gap (based upon the number of surviving particles as a function of time):

a transient phase, a gravitational relaxation phase, and a Lagrangian/niche phase. Furthermore, we developed a kinetic theory to describe the expected e-folding times for the first two of these phases. Because of the different orbital periods and mass ratios of the neighboring perturbers, we expect to find significant differences in the evolution of the Saturn/Uranus zone—as well as the Uranus/Neptune zone—in comparison with the Jupiter/Saturn zone

In Fig. 3, we plot the number of surviving planetesimals as a function of time for the Saturn/Uranus zones. The first phase, what wc have termed the "'transient phase." extends from the beginning of the simulation to 1.0x 10^5 years. In this phase, the bulk of the particles removed from the simulation are initially situated in the wings of the distribution and are removed by interacting with the activity spheres of the neighboring planets by differential rotation. A lesser effect is that many of the very eccentric particles throughout the distribution, regardless of initial sernimajor axis, are terminated during this phase.

Based on this argument, we expect the collision frequency ν to vary as nuAv where n is the number density of colliders (i.e., the Jovian planets), σ is the "collision cross section" of the collider, 'namely πR^2 where R **is** the radius of the two activity spheres, and Au is a measure of the velocity difference between planetesimal and planet (Sommerfeld, 1956). We used a weighted geometric mean of the activity radii of Saturn (0.36 AU) and Uranus (0.35 AU) —weights appropriate to the ratio of the number of particles removed by Uranus to those removed by Saturn. Taking that ratio to be 1..5 (see Table 1), we use $R = R_{Uranus}^{3/5} \times R_{Saturn}^{2/5}$. R had the value of 0.35 AU.

The number density is estimated from the volume appropriate to our initial planetesimal distribution (see above quantification for initial planetesimal distribution and details of computation method given in Paper I), and has the form of a torus extending between the orbits of the two adjoining planets. subtending an angle normal to the invariable plane with respect to the sun of= 40° (chosen to include 95% of the initial population). We calculated the corresponding volume to be

$\approx 9136\,AU^3$. Because the circular velocity $v \propto a^{-1/2}$, where a is the semimajor axis. we estimated the differential velocity Δv according to the velocity difference between a planet at the center of an activity sphere and a planetesimal on a circular orbit at its periphery. hence $\Delta v \approx (\Delta a/2a)v$, where $\Delta a = R_{act}$. For the Saturn/Uranus zone, we obtained $\Delta v \approx 2.1 \times 10^{-2}$ AU/yr. Combining these quantities yields an approximate e-folding time, i.e.. the reciprocal of v, of 5.5×10^5 yr while the computational result was 3.5×10^5 yr.

In the second phase, gravitational relaxation, the wings of the particle distribution are replenished as planetesimals undergo a form of random walk in momentum space, undergoing intermittent gravitational boosts as they migrate among the Jovian planets. The process of gravitational relaxation was first developed by Chandrasekhar (1943) and was elaborated upon in a major way for general Coulomb interactions by Spitzer (1962). More modern treatments of gravitational interactions on a planetesimal swarm can be found in Stewart and Kaula (1980) and Stewart and Wetherill (1988).

We can employ the Virial Theorem to help us determine the time scale associated with this process—describing the length of time required for a particle to undergo a major deflection by a planet. We relate Δv to the effective interaction distance r between a planetesimal and a planet of mass M, namely $GM/r \approx \Delta v^2$. Accordingly, we replace the "hard sphere)' cross section σ introduced above by the velocity-dependent version $\sigma_{\Delta v}$ according to $\pi r^2 \approx \pi (GM/\Delta v^2)^2$. Then. the appropriate time scale τ varies as $\Delta v^3/\pi n (GM)^2$. This expression shows us that gravitational collision times are smallest when Δv is smallest; hence. planetesimals that closely flank the activity spheres are among the first to be deflected into the path of these spheres of influence. We noted in the initialization section that the particles in this simulation initially had a Gaussian distribution with respect to their semimajor axes. Planetesimals closer to the center of the Gaussian distribution require much more time to complete their random walk into the path of a moving activity sphere.

We estimate the lifetime of those particles that must undergo the greatest change in Δv.

We first, calculated the velocity of a particle on a circular orbit halfway between Saturn and Uranus. v_{circ} = 1.66 AU/yr, then approximated Δv by $\Delta v \approx (\Delta a/2a)\, v$. Our average Δv was 0.56 AU/yr. Because we wish to consider gravitational scattering by either Saturn or Uranus. we will employ a weighted geometric mean of their GM values, weighted as were the activity radii for the transient phase, giving 3.7 x 10^{-3} AU^3/yr^2. We obtain, therefore, a gravitational relaxation time scale 1.9 x 10^7 yr, in comparison with our empirical value of 6.4 x 10^7 yr.

We observe here that by the end of the simulation, the system is making the transition to the third phase, but for the most part the Lagrangian/niche phase is conspicuously absent. We attribute this to two reasons. Firstly, 10^9 years is not sufficient time for the full gravitational relaxation of the Saturn/Uranus zone. Also, for our planetesimals, the initial Gaussian distribution in semimajor axis is such that the tails lie at the orbits of Saturn and Uranus. Cornpared to our Jupiter/Saturn survey, the particle density near the wings is rarefied-we have employed ten times fewer particles over nearly twice the semimajor axis range. Our initial conditions mitigate against 'Saturn or Uranus co-orbiters. Had the system reached full gravitational relaxation (i.e., which perhaps might emerge had the integration been continued to the age of the solar system), we are not convinced that the third phase would have manifested.

For the first two phases, our kinetic theory yields reasonable order-of-magnitude estimates, but in our Jupiter/Saturn investigation, agreement was substantially better. One possible explanation here is the consequence of our employing a factor of 10 fewer particles. However, we believe that the other planets, particularly Jupiter, have an especially important role in the Saturn/ Uranus zone. In addition to Saturn and Uranus, this zone is host to a nest of resonances from both Jupiter and Neptune—these resonances effectively scatter particles throughout the solar system. see Table 1.

Evidence for this can be seen in Fig. 4. We have grouped the particles by initial semimajor axis in 0.2 AU intervals and sorted the particles in each interval with respect to lifetimes. The high and low values represent the first and third quartiles respectively. Along the bottom of the figure, we indicate the positions of low-order mean motion commensurabilities of Jupiter and Saturn, while across the top, we show commensurabilities with Uranus and Neptune (the values of which we list in Table 1). The location of mean motion commensurabilities that we have indicated are those at the start of the simulation and do not reflect short- and long-term variations of the semimajor axes of any of the planets.

In Fig. 4, we observe rapidly depleted bands whose existence would be difficult to explain as the combined effect of Saturn and Uranus alone. For example, the region from 12.6 to 13.2 AU is a band in which the particle lifetimes are relatively short. The position of this band is not easily explained when we look at Saturn and Uranus alone, but we see that the Jupiter 1:4, and perhaps to a lesser extent the Neptune 7:2 resonance, seem to have aided in clearing this band of planetesimals. This seems to confirm the conclusion in GD90 that, in order to capture the dynamics of the solar system, any simulation must necessarily include all of the Jovian planets

Figure 4 also clearly indicates that, with the exception of a band centered at 14.2 AU, the overwhelming majority of the particles in this region are depleted within 10^7 years. If over the span of their lifetimes, the planets (particularly Uranus and Neptune) migrated either sunwards (Kaula and Newman 1990), or anti-sunwards (Fernandez and Ip, 1981, 1983, 19S4: Malhotra 1994). as a result of interactions with a planetesimal swarm with nonnegligible mass, the positions of these resonances would have "scanned" (c f.. Ward, 1981) accordingly. thus sweeping out these regions even more rapidly than indicated in this simulation.

Further evidence for the role of Jupiter in the Saturn/Uranus zone is apparent in Fig. 5. where we plot the average (plus/minus one standard deviation) semimajor axis of all particles

removed from the simulation in .5000 -year intervals. In our Jupiter/Saturn study. a similar plot was consistent with a population that was initially depleted at its wings, with a subsequent winnowing symmetrically inwards. In the Saturn/Uranus zone, we see an apparent asymmetry. particularly in the first 5000 years, where the average semimajor axis is skewed towards Saturn. Returning to Fig. 4, we can see a similar asymmetry in which particles that begin closer to Saturn are, in general, shorter-lived that those that began near Uranus. 'I'he mass difference between Saturn and Uranus alone is probably not enough to cause this disparity.

In Table 2 we indicate the relative importance of various mechanisms for depleting particles from the Saturn/Uranus zone according to the planetesimals' initial semimajor axes. In each 0.2 AU interval, we enumerate how many test particles survived until the end of the simulation, how many were eliminated through collision with the activity spheres of the Jovian planets, and how many were ejected from the solar system. In our Jupiter/Saturn study, we found that the ratio of particles eliminated by Saturn to that of Jupiter was basically uniform and explicable by simple geometrical-kinetic arguments. Here we see a much more intricate pattern that no longer preserves the ratios and that show a pronounced asymmetry, which we attribute to the symmetry-breaking influence of Jupiter, and again to a lesser extent. Neptune. Also in our Jupiter/Saturn study, we found that a greater number of particles were eliminated by interaction with the activity sphere of the outer planet, rather than by the inner. In Fig. 6 we plot the number of particles eliminated by Jupiter and by Saturn as a function of initial semimajor axis range—we have plotted the Jupiter/Saturn equivalent of columns two and three of Table 2. This plot yields two Gaussian-like curves, peaked at 6.98 AU (particles eliminated by Jupiter) and 7.54 AU (particles eliminated by Saturn), to which we have fit Gaussian functions in order to determine where the curves are peaked. The peak-to-peak distance is 0.56 AU within an overall range of 4.8 AU. In Fig. 7 we present a similar plot for the Saturn/Uranus zone. indicating the number of particles eliminated

through interaction with the neighboring planets. Again. we see two Gaussian-1ike curves with the outer planet eliminating the majority of the planetesimals. As with Fig. 6. we have plotted the best-fit Gaussian function through the curves to determine where the data are peaked. In Fig. 7 the peaks of the two curves, at 13.3 and 1.5.1 AU have been pulled apart to a distance of 1.8AU versus a 9.7 AU range. This, again, is almost certainly due to the combined effects of Jupiter and Neptune.

Complementary to Table 2 is Table 3, in which we present the mean and standard deviation of initial and final semimajor axes for all particles eliminated by the activity spheres of the Jovian planets. The first thing we note is that, consistent with our Jupiter/Saturn study, we see a migration of the planetesimals outwards. Particles terminated by collision with the activity sphere of Uranus had semimajor axes that were, on average, nearly 1 AU greater than that with which they began the simulation. Even particles terminated by Saturn had, on average, greater final semimajor axes than initial.

In Table *4, we* enumerate the number of particles that ended the simulation with their semi-major axes in various ranges. Particles with semimajor axes between 5.2 and 9.5 AU ended the simulation in the Jupiter/Saturn zone; however, this accounted for less than 3 percent of our sample. The bulk of the particles, nearly 93%, were situated between 9.5-and 19.2 AU when they were terminated—still in the Saturn/Uranus zone. Despite the general trend of the particles to migrate outwards during the simulation, less than .5 percent ended up in the Uranus/Neptune zone. only 18 planetesimals had semimajor axes beyond that, including one ejection.

In order to visualize the effect of initial inclination on planetesimal lifetimes. we present Fig. 8–remaining planet esimals as a function of time for particles of 0° to 0.5°. 5° ± 0.5°. 10° ± 0.5°. 15° ± 0..5°. and 20° ± 0.5° inclinations. In the Saturn/Uranus zone, we see that more highly inclined particles generally have increased lifetimes. This is, however, as would be expected. Any planetary

perturbations to low-inclination particles would directly modify the magnitude of the particle's angular momentum. For inclined cases, such perturbations have both an in-plane and out-of-plane component, and affect the orientation of particle's angular momentum vector (i.e.. its inclination) in addition to its magnitude. One implication of this is that mean motion resonances with the Jovian planets would be much more efficient in "pumping up" the eccentricities of low-inclination planetesimals than those at higher inclinations.

In Fig. 9, we plot the mean inclination in degrees, plus/minus one standard deviation, of all particles terminated within 5000-year windows. Unlike our Jupiter/Saturn study, we see no clear upwards trend.

Table *5* yields an indication of the relative significance of various mechanisms of depleting the planetesimal swarm as a function of initial planetesimal inclination. In each 1° range, we indicate the number of planetesimals that were eliminated by the activity spheres of the Jovian planets, how many were ejected from the solar system, and how many survived the entire integration. In our Jupiter/Saturn study we sought to explain, through a simple geometric argument, not only why more particles were eliminated through interaction with Saturn's activity sphere as opposed to Jupiter's, but the ratio as well. We assumed that the annulus a planet's activity radius sweeps out in an orbit was a target—the ratio of the areas of these annuli should yield a reasonable "back of the envelope" estimate of the ratio of the number of particles eliminated by the activity spheres of the neighboring planets. Using a similar argument. we would expect Uranus to be responsible for eliminating approximately twice the number of particles as does Saturn. In reviewing Table 5, we see that this estimate does not work nearly as well as it did for the .Jupiter/Saturn zone. and that. for particles inclined up to 20°, the actual ratio varies from 1.84 down to 1.12. We can attribute this to two factors. First, we are dealing with a sample size one tenth that of our Jupiter/Saturn study. and our uncertainties are certainly higher. More probable is the fact that

resonant effects with all the Jovian planets have the effect of pumping up the eccentricities of a substantial fraction of the particles so that they cross the orbits of both Saturn and Uranus. This would explain why we see a general outwards migration in the semimajor axes of the particles. yet Saturn is responsible for removing a greater-than-expected number of particles.

The role of initial eccentricity on particle lifetimes can be see in Fig. 10. Here we examine the number of particles remaining as a function of time for initial eccentricities of 0.00 + 0.02.5, 0.05 ± 0.02.5, 0.10 ± 0.025, 0.1.5* 0.025, and 0.20* 0.02.5. Particles which are more eccentric at the onset of the simulation are, in general, much more shorter-lived than those on more circular orbits. This is as would be expected, and is as we have seen in our previous study. Further evidence of this is shown in Fig. 11. Here we have shown t he average initial eccentricities (plus/minus one standard deviation) of particles eliminated in 5000-year periods. Again, we see that particles on more eccentric orbits are eliminated sooner. Similar to our Jupiter/Saturn study, we see a decrease in the mean number of particles eliminated in 5000-year periods as the simulation progresses, consistent with Fig. 8, in which we see that the more eccentric particles are terminated early on.

Figure 12 reveals the first-order evolution of the Saturn/Uranus zone for the first 6 My. We have plotted the number of surviving particles as a function of initial semimajor axis in 1 My increments ranging from the beginning of the simulation up to 6 My. The lines at the top of the figure indicate both the locations of the resonances which manifest in this region. while the lengths indicate their comparative orders, in Roy (1982, p. Ml)-)—the longer the line. the more important (or lower in order) the resonance. This figure represents only a first-order indication of the system evolution-we have examined the number of particles surviving at different times in the simulation as a function of their *initial* semimajor axis—the orbits of many particles will have certainly been altered over time. Nevertheless. we clearly see the system quickly evolve into both rapidly-depleted and long-life bands. The depleted band at 15 AU corresponds to the Saturn

1:2 mean motion commensurability. However. we observe that Saturn's 2:3 resonance. which is at *12..5 AU,* appears stable. Do we have "Plutos"? We also see a more subtle effect from the Uranus 3:2 and 4:3 commensurabilities at 14.7 and 15.9 AU, respectively. Though this represents only the early evolution of the Saturn/Uranus zone, we can easily identify three, arguably four, long-life bands centered at 12..5, 14.4, 15.5, and 16 AU.

At the end of the simulation, however, only one particle survived the entire 1 By integration. This particle had a semimajor axis of 12.48 AU (just inside the Saturn 2:3 resonance), an eccentricity of 0.055, and an inclination of 1.53°. Though only one particle survived the entire integration. we found three bands of long-lived particles, stable over 100 My time periods, centered at 12.5, 14.4, and 16 AU. Plotted in Fig. 13 is the final semimajor axis versus eccentricity of the particles, 135 in all, which survived the first 100 My of the integration. 'The band at 14.4 AU is interesting in that it contains nearly 100 of the 135 remaining planetesimals. In a search for stable orbits in the Saturn/Uranus zone over solar system lifetimes, this band is probably the best candidate for a more focused search. Taking into consideration the roles of eccentricity and inclination on planetesimal lifetimes, such a search would be most efficient were it confined to nearly circular orbits over a range of inclinations, Again we make the caveat that if the planetesimal swarm was comprised of particles of nonnegligible mass. the planets themselves may have migrated, their mean motion commensurabilities would have "scanned, " and it is likely that any long-life bands we find in this simulation would be stable for periods much shorter than our results suggest. Now we turn our attention to the Uranus/Neptune zone, which, as we will shortly see, shows some significant, differences as well as some remarkable similarities.

The Uranus/Neptune Zone.

In Fig. 14 we plot the number of surviving planetesimals as a function of time for our Uranus/Neptune zone survey. As with the Saturn/Uranus zone, we find that the system is in tran-

sition to the third phase of evolution that we described in our Jupiter/Saturn study-indicating that, like the Saturn/Uranus zone, 10^9 years is not sufficient time for full gravitational relaxation of the Uranus/Neptune zone.

Similar to Saturn/Uranus above, we have estimated the expected lifetimes of particles in the Uranus/Neptune zone using a basic kinetic theory. For the phase that we have termed the "transient" phase, we use a toroidal volume of 30300 AU^3. To estimate the average cross-sectional area of the colliders, we used the weighted geometric mean of the activity radii of Uranus ($\approx$ 0.35 AU) and Neptune (≈ 0.58 *AU)* to approximate R, where $R = R_{Neptune}^{3/5} R_{Uranus}^{2/5}$, and the value of 0.46 AU, giving a cross section of 0,67 AU^2. To estimate Δv we used the mean difference between the planetary velocities and particles orbiting at their periphery, 1.7x 10^{-2} AU/yr. Using these values in the equations given above, we find a theoretical time scale for the transient phase in the Uranus/Neptune zone of 1.34 x 10^6 yr; the computational result was 1.57 x 10^5 yr. Of all our estimates for depletion rates this had, by far, the greatest error. We suggest a reason for this below.

The gravitational relaxation phase describes the length of time required for a particle to undergo a major deflection by a planet. Again, the first step is to calculate the velocity-dependent collisional cross section. To estimate Av we first calculated the velocity of a particle on a circular orbit halfway between Uranus and Neptune. v_{circ} = 1.27 AU/yr, then approximated Δv by $\Delta v \approx (\Delta a/2a)v$. Our average Δv was 0.28 AU/yr. For GM we used the weighted geometric mean of GM_{Uranus} and $GM_{Neptune}$, 1.9 x $10^{-3} AU^3/yr^2$. Hence, for the relaxation phase, our theoretical estimate was 2.9 x 10^7 yr; the simulation value was 5.9 x 10^7 yr. As with Saturn/Uranus. our theoretical estimates for e-folding times for the Uranus/Neptune zone are not as near in agreement with the computational results as were those for Jupiter/Saturn.

It is noteworthy that all of the time scales, for both the Saturn/Uranus and Uranus/Neptune

cases, are much longer than in the corresponding Jupiter/Saturn cases, by as much as a factor of 380. Interestingly, the simulation e-folding times for the Uranus/Neptune zone were actually smaller than those for the Saturn/Uranus zone, suggesting that the Uranus/Neptune zone was. in general, more rapidly evacuated.

In Fig. 15, we examine the expected lifetimes of particles in the Uranus/Neptune zone as a function of their initial semimajor axis (in 0.2 AU intervals). As with Fig. 4, we have indicated the position of several Jovian planet mean motion commensurabilities. Jupiter and Saturn resonances are indicated across the bottom of Fig. 12, and those with Uranus and Neptune at the top—the semimajor axis values for these are indicated in Table 6. In Fig. 12, as with Fig. 4, we see the bulk of the particles are removed from this zone on 10^6- to 107-year time scales.

We note two bands, at 23 and 25 AU, where mean motion commensurabilities appear to have dramatically decreased planetesimal lifetimes. The effect of Jupiter and Saturn on this zone does not appear to be as pronounced as the effect of Jupiter and Neptune on the Saturn/Uranus zone, as could have been expected. The short-life band at 25 AU is coincident with the Neptune 4:3 and Uranus 2:3 commensurabilities. Figure 15 also suggests that t here was a long-life band centered at 26 AU, in agreement with results from similar previous studies.

In both the Jupiter/Saturn and Saturn/Uranus studies we examined 'the statistics of the particles removed from our simulation over .5000-year periods. For Jupiter/Saturn, the mean semimajor axis plus or minus one standard deviation was consistent with a population that was winnowed symmetrically inwards: for Saturn/Uranus we noted an asymmetry in this population that seemed to indicate that particles closer to Saturn. i.e.. those with smaller semimajor axes. were preferentially eliminated—possibly owing to the role of Jupiter. In Fig. 16 we see no evidence of either type of trend for the first 10^5 years.

In Table 7 we examine the termination mechanisms for all particles as a function of their

initial semimajor axes, in 0.2 AU increments. Consistent with both the Jupiter/Saturn and Saturn/Uranus zones, we see that collisions with the outer planet's activity sphere, in this case Neptune, is responsible for removing the bulk of the particles. This is consistent with our earlier two simulations in which we saw a genera] outwards migration of the particles, and, in fact, only 18 particles were removed by Jupiter (2) and Saturn (16). Only two particles were ejected from the solar system, both of which had inclinations of less than one degree. In their simulation of the Uranus/Neptune zone, SW84 reported that the "vast majority" of their planetesimals were ejected from the solar system. We saw only two ejections, but SW84 modeled close pianet/planetesimal encounters-we did not. On the other hand, Weissman (1994) has argued that neither Uranus nor Neptune has the gravity to eject a significant number of comets from the solai system, so perhaps the high percentage of ejections seen by SW84 were an artifact of their numerical methods.

In Fig, 17 we plot the number of planetesimals eliminated by the nearest-neighbor planets, as a function of initial semimajor axis, and as with Fig. 6 and Fig. 7 we have fit Gaussian functions through these curves. We see two peaks, at 23.6, and 25.3 AU, with the outer planet responsible 'for the elimination of more planetesimals. The peak-to-peak distance in this plot is 1.7 AU over an 11 AU range. Taken together, Figs. 6, 7, and 17 would seem to indicate that Uranus and Neptune had a trivial effect on the dynamics of the Jupiter/Saturn zone, but the combined effect of Jupiter and Neptune on the Saturn/Uranus zone pulled apart the peaks we see in Fig. 7. In the Neptune/Uranus zone, we see the two peaks intermediate in distance between those in the Jupiter/Saturn and Saturn/Uranus zones, suggesting that the combined effect of the inner Jovian planet had a lesser, though nontrivial, effect on the dynamics of the Uranus/Neptune zone than in Saturn/ Uranus.

Table 8 depicts the mean and standard deviation of initial and final semimajor axes for all particles eliminated by the activity spheres of the four planets. Because the particles eliminated

by Jupiter and Saturn represent a statistically insignificant subset of the population, we will focus only on those eliminated by Uranus and Neptune. We see that, on average, the particles eliminated by the activity sphere of Uranus migrated approximately 0.6 AU inwards, but those eliminated by Neptune migrated 1.2 AU outwards. Because Neptune was responsible for eliminating: more planetesimals than Uranus, again we see a general outwards migration. This effect is corroborated by Table 9, in which we list the number of particles that fell into various semimajor axis ranges at the time of their removal from the simulation. Compared to our Jupiter/Saturn and Saturn/Uranus studies, a much greater percentage of particles in the Uranus/ lNeptune zone finished their lives having semimajor axes in the interplanet zone in which they began the simulation. This is almost certainly due to the comparatively smaller gravitational pull of the neighboring perturbers, along with the much greater distance scales over which these perturbations acted. We see that less than 1..5% of the particles evolved sunwards, and approximately 3.6% had semimajor axes greater than that of Neptune. Nearly 95% of the particles were terminated while still, strictly speaking, in the Uranus/Neptune zone.

The particles in this zone were more "confined" than in our Jupiter/Saturn and Saturn/Uranus simulations (i.e., a greater percentage of particles were eliminated while having their semimajor axes still in their original zone). Because a higher percentage of particles in the other two studies migrated outside their initial zones, this functionally increased the volume of their "container. " and this would argue that our kinetic theory would have been in *closest* agreement with the actual simulation rates for the Uranus/Neptune zone—instead, agreement with a simple kinetic theory was worse for the zone between the outer two planets.

We suggest that the reason for this is a combination of our choice of initial conditions. and the location of a low-order mean motion resonance which manifests in this zone. Our initial particle ensemble was Gaussian-distributed in semimajor axis so that the peak of the distribution was

located half way between neighboring Jovian planets. In the Neptune/Uranus case, the peak of this distribution was at 24.6 AU; the Neptune 4:3 resonance is at 24.8 AU . Indeed. throughout the Uranus/Neptune zone, low-order commensurabilities are more evenly distributed, rather than "clumped" as in the Saturn/Uranus zone, so we don't see such dramatic peaks in particle lifetimes as we did at 14.4 AU in the Saturn/Uranus zone. The Jupiter/Saturn zone is so dynamically unstable from the gravitational "stirring" of the two largest Jovian planets that. even though we clearly saw decreased particle lifetimes at the Jupiter 2:3 and Saturn 3:5 resonances, it is very likely that resonant effects had a greater relative influence in depleting the Saturn/Uranus and Uranus/Neptune zones. It is likely that this is especially true when the Neptune 4:3 resonance manifests itself very near to a substantial fraction of the initial distribution.

This effect would not only explain the order-of-magnitude error in our kinetic theory estimate of the Uranus/Neptune transient phase depletion rate, but would also explain why the Neptune/Uranus zone was depleted more rapidly than the Saturn/Uranus gap. In the Saturn/Uranus zone, the peak of the distribution (14.4 AU) was very near the long-life band we reported centered -at 14.2 AU. Not only were a large number of Uranus/Neptune zone planetesimals initially situated in a rapidly depleted band, but a similarly large number of Saturn/Uranus planetesimals were initially located in a long-life band. This would also explain why over twice as many. Saturn/Uranus zone planetesimals survived beyond 100 My (13.5) than Uranus/Neptune particles (61). We discuss this further below.

As we have done in our previous two studies, we show a "family of curves" in Fig. 18. depicting the comparative depletion rates of particles as a function of their initial inclinations. The tolerance ranges for each curve are the same as for our Saturn/Uranus simulation. Unlike our two previous studies. however. Fig. 18 yields two surprises. The first is that in the first .5x 10^5 years of simulation time, planetesimals very near to the invariable plane have a *much* higher depletion rate than those

which are inclined even as little as .5°.

In hindsight, this may not be surprising after all. As we have already pointed out, the eccentricities of low-inclination planetesimals are increased more readily by resonant effects than the eccentricities of more highly inclined bodies. We have also seen that the Neptune 4:3 resonance may have been responsible for the elimination of a greater-than-expected number of particles during the transient phase of evolution. It is logical, then, that this, and other commensurabilities preferentially affected low-inclination planetesimals, causing an increased depletion of bodies near the invariable plane.

The second surprise is that by 5 $x\,10^6$ years, the zero-inclination curve crosses the 5° and 10° curves. The very long-lived planetesimals, then, are either close to the invariable plane, or very highly inclined. In Fig. 19, we plot the mean inclination in degrees, plus or minus one standard deviation," of all particles terminated within 5000-year windows. Here we see a clear upwards trend, consistent with Fig. 18, showing that low-inclination particles are rapidly eliminated from the simulation at the onset.

In Table 10, as with Table 5, we enumerate the comparative elimination mechanisms of particles as a function of initial inclination in 1° increments. .4s with our previous two studies, we see that the outer planet is responsible for eliminating more planetesimals than the inner planet for all inclination ranges, except for the very high inclinations that show the effects of small number statistics.

In Figs. 20 and 21 we examine the role that initial eccentricity had on particle depletion rates and find no surprises. Figure 20 is another family of curves whose parameters are the same as those in Fig. 8. Here we see once again that more eccentric particles are eliminated more quickly. Figure 21, a plot of mean eccentricities, plus or minus one standard deviation. of particles eliminated over .5000 -year periods. also indicates that the longer-lived planetesimals began the simulation with more

circular orbits, though the downwards trend is not nearly as pronounced as in the Saturn/Uranus zone, nor the Jupiter/Saturn zone.

Figure 22, as with Fig. 12, shows the evolution of the Uranus/Neptune zone to first order. Qualitatively, we see a much different picture than for the Saturn/Uranus zone. In the Saturn/Uranus zone, we saw how very strong mean-motion commensurabili ties almost completely deplete bands on very short time scales, although there are numerous particles in other long-life bands. In the Uranus/Neptune zone, we see neither the very unstable stable bands, nor clo we see large numbers of particles in very stable bands. Instead, we see hints of weaker resonances eroding the planetesimal swarm in a more symmetric fashion. As with Fig.15, we observe a depleted band at 22.6 AU, probably as a result of the Neptune 3:2 resonance. We see another centered at 25.2 AU, corresponding to the Uranus 2:3 and the Neptune 4:3 resonances. There are also hints of resonant effects at 21.8 AU (Uranus 5:6), 24.0 AU (Uranus 5:7 and Saturn 1:4), and 26.4 AU (Uranus 5:8). We also see hints of long-life bands at 22.4, 23.2, 24.5, and 26 AU. In Fig. 23, we show the semimajor axis and inclination of all particles that survived the simulation beyond 100 My. Here we see that there are two long-life bands—centered at 24.5 AU and 26 AU—in the Uranus/Neptune zone, in agreement with results of previous investigations. There is also the suggestion of a long-life band at 22.5 AU. Four particles survived the first 100 My in orbits nearly commensurate with Neptune, One of these four particles was the only particle in the simulation to survive the entire 1 By integration time. HW93 showed that particles situated at Neptune's triangular Lagrange points were stable for up to 20 My. here we see evidence that they are stable for much longer periods of time.

5. CONCLUSIONS

This. then. concludes our investigation of the Saturn/ Uranus and Uranus/Neptune zones. The most important outcome of this study, relevant to our solar system's origin. is that niches for

primordial planetesimal material between the Jovian planets will be. if not nonexistent, few and far between. Consistent with other studies, we find long-life bands between the outer planets centered at 12..5, 14.4, 16.0, 24.5, and 26.0 AU. Particles in these bands may be stable on time scales of up to 10^8 years. Only two planetesimals out of 20,000 survived the entire 1 By integration; however. one in each of the Saturn/Uranus and Uranus/Neptune zones. One of these particles was a Neptune librator, indicating that planetesimals orbiting at the triangular Lagrange point of Neptune may be stable over long time periods. On the other hand, if early in their lifetimes, the outer Jovian planets migrated to their present locations, it is unlikely that either of these orbits would be stable over billion-year time scales.

In comparison with our Jupiter/Saturn study, we see that the time scales relevant to the dynamical evolution of the outer solar system are truly different! In the Jupiter/Saturn zone, planetesimals were eliminated on 10^4- to 105-year time scales. Particles in both the Saturn/Uranus and Uranus/Neptune zones survived much longer, on average, and were eliminated on 10^6- to 10^7-year time scales.

In our simulations, the Neptune/Uranus zone was depleted more rapidly than the Saturn/Uranus zone, but this was very likely because of the fact that our initial conditions place a large number of Uranus/Neptune zone particles in locations strongly affected by more mean motion resonances. This, perhaps. may also explain why our kinetic theory estimate of planetesimal depletion rates was in much better agreement in both our .Jupiter/Saturn and Saturn/Uranus zone studies. Resonant effects may have also preferentially depleted the Uranus/Neptune zone of low-inclination particles. In comparison to the .Jupiter/Saturn zone, resonant effects appear to have had a greater comparative effect in both of these regions than did "'gravitational stirring. "

The planetesimals in our simulation underwent a general outwards migration. This is consistent with the results of our Jupiter/Saturn zone study and with the results of researchers who

have performed computational studies of galaxy dynamics and have seen such a "'mass segregation" (Farouki and Salpeter, 1982; Farouki et al.. 1983; Spitzer, 1987). The results of other dynamical simulations of the outer solar system have indicated that planetesimals situated between the three outer planets may, in fact, have migrated *inwards* (Fernandez and Ip, 1981, 19S3, 1984) These studies, however, included particles of nonnegligible mass, and modeled planet /planetesimal close encounters.

Acknowledgments: The authors would like to thank John W. Dunbar of Hughes Aircraft Corporation and Norman Field at UCLA for their computational assistance. We are particularly grateful to Ferenc Varadi for many helpful discussions. The research described in this paper was carried out in part at the Jet Propulsion Laboratory, California Institute of Technology, and was supported by NASA grant NAGW 3132.

REFERENCES

Arnold, J. R. 1965. The Origin of Meteorites as Small Bodies. H. The Model *Astrophys. J.* 141, 1536–1.547.

Bell, R. E., K. R. Grazier, W. I. Newman, W. M. Kaula, and J. M. Hyman, 1994. Long Term Integrations of the Solar System: Simplicity Beats Symplecticity, 24th DDA meeting, Kingsville, TX—*B.A.A.S.* vol 26, no. 2.

Bus, S. H., M.F. A'Hearn, D. G. Schleicher, E. Bowell, 1991. Detection of CN Emission from (2060) Chiron. Science 251, 774-777.

Candy, J., and W. Rozmus 1990. A Symplectic Integration Algorithm for Separable Hamiltonian Functions. J. *Comput. Phys. 92, 230-256.*

Chandrasekhar, S. 1942. Stochastic Problems in Physics and Astronomy. *Rev. Mod. Phys.* 15, 1-89.

Chandrasekhar, S. 1943. *Principles of Stellar Dynamics* (Chicago: University of Chicago Press).

Chapman, S. and T. G. Cowling 1970. *The Mathematical Theory of Non-Uniform Gases.* Third Edition (Cambridge: Cambridge University Press *j.*

Cohen, C. J., E. C. Hubbard, and C. Oesterwinter 1973. Astron. Papers Amer. Ephemeris. 22.

Danby, J. M. A.. 1988. *Fundamentals of Celestial Mechanics.* Second Revised Edition (Richmond. Viginia: Willmann-Bell).

de 1a Barre, C'. M., W. M. Kaula, and F. Varadi1996. A Study of the Orbits near Saturn-s Triangular Lagrangian Points. *Icarus* 121 88-113.

Duncan. M.. T. Quinn, and S. Tremaine 1989. The Long-Term Evolution of Orbits in the Solar System: A Mapping Approach, *Icarus 82.* 402–418.

Duncan, M., and T. Quinn 1993. The Long-Term Dynamical Evolution of the Solar System. *Annu. Rev. Astron. Astrophys.* 31, 26.5-295.

Farouki, R. T., and E. E. Salpeter 1983. Mass Segregation. Relaxation. and the Coulomb Logarithm in N-body Systems. *Ap.* J., 253, 512–.519.

Farouki, R. T., G. L. Hoffman, and E. E. Salpeter 1983. The Collapse and Violent Relaxation of *N*-body Systems: Mass Segregation and the Secondary Maximum. *Ap. J.*, 271. 11-21.

Fernandez, J. A., and W. -H. Ip 1981. Dynamical Evolution of a Cometary Swarm in the outer Planetary Region, *Icarus* 47, 470-479.

Fernandez, J. A., and W. -H. Ip 1983. On the Time Evolution of the Cometary Influx in the Region of the Terrestrial Planets, *Icarus* 54, 377-387.

Fernandez, J. A., and W. -H. Ip 1984. Some Dynamical Aspects of the Accretion of Uranus and Neptune: The Exchange of Orbital Angular Momentum with Planetesimals. *Icarus* 58, 109--120.

Giorgini, J. D., D.K Yeomans, A. B. Chamberlain, P. W. Chodas, R. A. Jacobsen, M. S. Keesey, J. H. Lieske, S. J. Ostro, E. M. Standish, and R. N. Wimberly, 1996. Horizons: JPL's On-Line Solar System Data Service, to appear in *B.A.A.S.*.

Gladman, B. and M. Duncan, 1990. On the Fates of Minor Bodies in the Outer Solar System, *Astron. J.* 100, 1680-1693.

Grazier, K. R., W. I. Newman, W. M. Kaula, F. Varadi, and J. M. Hyman, 199.5. An Exhaustive Search for Stable Orbits in the Outer Solar System, 25th DDA meeting, Yosemite, CA— *B.A.A.S.* vol 24, no. 2,

Grazier, K. R., W. I. Newman, W. M. Kaula, and J. M. Hyman, 1996. Statistical Mechanics and Dynamics of the Outer Solar System. I. The Jupiter/Saturn Zone. Submitted *to Icarus.*

Hairer, E., S. P. Nøorsett, and G. Wanner 1991. Solving *ordinary Differential Equations I: Nonstiff Problems,* Second Revised Edition (Berlin: Springer-Verlag).

Henrici, P. 1962. *Discrete Variable Methods in Ordinary Differential Equations (New* York: John Wiley & Sons).

Higham, N. J. 1993. The Accuracy of Floating Point Summation, *SIAM J. Sci. Comput.* 14, 783-799.

Holman, M. J. and J. Wisdom, 1993. Dynamical Stability in the Outer Solar System and the Delivery of Short Period Comets, *Astron. J.* 105, 5, 1987-1999.

Levison, H. F. and M. J. Duncan 1993. The Gravitational Sculpting of the Kuiper Belt. *Ap. J. Lett. 406.* L35–L38.

Meech. K. J.. and M. J. S. Belton. *IAU Circ.* No. 4770, April 11, 1989.

Newman. W. I., M. P. Haynes. and Y. Terzian 1989. Double Galaxy Redshifts and the Statistics of Small Numbers, *Ap. J.* 344, 111–114.

Newman, W. I.. E. Y. Lob, W. M. Kaula. and G. D. Doolen 1990. Numerical Stability and Round-off Properties of Cowell-Störmer Type Integration Methods, *Bull. Amer. Astro. Soc. 22.* 950.

Newman. W. I., M. P. Haynes, and Y. Terzian 1992. Limitations to the Method of Power Spectrum Analysis: Nonstationarity, Biased Estimators, and Weak Convergence to Normality. E. D. Feigelson and G. J. Babu, eds., *Statistical Challenges in Modern Astronomy* (New York: Springer-Verlag), (137-1.53, 161-162).

Newman, W.L., W.M. Kaula, J. M. Hyman, J.C. Scovel, E. N. Loh 1993. Simplicity beats Symplecticity, Paper Presented at the Workshop on Integration Algorithms for Classical Mechanics, Fields Institute for Research in Mathematical Sciences, Waterloo. ON, October 13-17.199:3.

Newman, W. I.. M. P. Haynes, and Y. Terzian 1994. Redshift Data and Statistical Inference, *Astrophys. J.*, 431, 147–1.5.5.

Newman, W. I., F. Varadi, K. R. Grazier, W. M. Kaula, and J. M. Hyman 1995. Mappings and Integrators on the Edge of Chaos, 2.5th DDA meeting, Yosemite. CA—*B.A.A.S.* vol 21. no. 2.

Newman, W. I., K. R. Grazier, W. M. Kaula, and J. M. Hyman 1997. Optimal Multistep Integrators for Second Order Ordinary Differential Equations, in preparation.

Nobili, .4. M., A. Milani, and M. Carpino 1989. Fundamental Frequencies and Small Divisors in the Orbits of the Outer Planets. *Astron. Astrophys. 210313--336.*

Öpik, E. J. 1976, *Interplanetary Encounters (New* York: Elsevier).

Press, W. H., B. P. Flannery, S. A. Teukolsky, and W. T. Vetterling 1988. *Numerical Recipes in C: The Art of Scientific Computing (New* York: Cambridge University Press).

Quinlan, G. D. 1994. Round-Off Error in Long-Term Orbital Integrations Using Multistep Methods, *Celest. Mech. Dyn. Astron. 58, 339–351.*

Roy, A. E., 1982. *Orbital Motion,* Second edition (Bristol, United Kingdom: Adam Hilger Ltd.).

Sanz-Serna, J. M. and M. P. Calvo 1994. *Numerical Hamiltonian Problems* (London: Chapman & Hall).

Shoemaker, E. M. and R. F. Wolfe 1984. Evolution of the Uranus-Neptune Planetesimal Swarm. *Lunar Planet Sci. Conf.*, 15, 780-781.

Spitzer, Jr., L. 1962. *Physics of Fully Ionized Gases,* Second Revised Edition (New York: Interscience).

Sommerfeld, A. 1956. *Thermodynamics and Statistical Mechanics.* Ed. F. Bopp, J. Meixner; translated by J. Kestin (New York: Academic Press).

-Stewart, G. R. and W. M. Kaula 1980. A Gravitational Kinetic Theory for Planetesimals, *Icarus 44, 154-171.*

Stewart, G. R. and G. W. Wetherill 1988. Evolution of Planetesimal Velocities, *Icarus 74, 542-53.*

Ward, W. R. 1981. Solar Nebula Dispersal and the Stability of the Planetary System. *Icarus 47, 234-264.*

Weissman, P. R. 1994. Why Are There No Interstellar Comets? 24th DDA meeting. Kingsville, TX—*B.A.A.S.* vol 20, no. 2.

Wisdom. J. and M. Holman, 1991. Symplectic Maps for the N-Body Problem, *Astron. J.* 102. 1.528-1538.

TABLE CAPTIONS

'Table 1. The location of Jovian planet mean motion commensurabilities that are manifested in the Sat, urn/Uranus zone.

Table 2. Depletion "mechanisms" for all Saturn/ Uranus planetesimals as a function of their initial semimajor axis range, in 0.2 AU increments.

Table 3. Initial and final mean semimajor axes, and standard deviations, of all Saturn/Uranus planetesimals eliminated by each of the Jovian planets. With the exception of the particles eliminated by the activity sphere of Jupiter, which was only 28 particles, we see an outwards migration in the semimajor axes of the planetesimals, even for those eliminated by Saturn.

Table 4 Here we indicate the comparative number of planetesimals whose sernimajor axes fell into various ranges of interest. Nearly 93% of the particles initially situated between Saturn and Uranus were still in this zone at the time of their elimination from the simulation. Just under 5% were in the Uranus/Neptune zone; just over 2% were between Jupiter and Saturn. Only three particles were kicked interior to Jupiter, and there was only one ejection.

Table .5. Depletion "mechanisms" for all Saturn/Uranus planetesimals as a function of their initial inclinations, in 1.0 degree increments.

Table 6. The location of Jovian planet mean motion commensurabilities that are manifested in the Uranus/Neptune zone.

Table 7. Depletion "mechanisms" for all Uranus/Neptune planetesimals as a function of their initial semimajor axis range, in 0.2 AU increments.

Table 8. Initial and final mean semimajor axes, and standard deviations, of all Uranus/Neptune planetesimals eliminated by each of the Jovian planets. The semimajor axes of particles eliminated by the activity spheres of Uranus and Jupiter showed an inwards migration, but those eliminated by Neptune and Saturn generally migrated outwards. Because Neptune was the planet that eliminated the majority of the planetesimals, we see a general outwards migration of planetesimals, consistent with our Jupiter/Saturn and Saturn/Uranus simulations.

Table 9. Here we indicate the comparative number of planetesimals whose semimajor axes "'fell into various ranges of interest. Nearly 95% of the particles initially situated between Uranus and Neptune were still in this zone at the time of their elimination from the simulation. Only 1.4% were in the Saturn/Uranus zone; just over 3.6% were exterior to Neptune. There were only two ejections.

Table 10. Depletion "mechanisms" for all Uranus/Neptune planetesimals as a function of their nitial inclinations, in 1.0 degree increments.

FIGURE CAPTIONS

Fig. 1. Relative RMS energy error for outer solar system foreward/back integration. Values are for times corresponding to 2° to 2^{18} orbits of Jupiter. Nonlinear power-law regression reveals a power law index of ≈ 0.46, indicating the absence of any significant systematic integration error.

Fig, 2. Absolute RMS longitude error of the Jovian planets for forward/back integrations using 16 different sets of initial conditions. Nonlinear power-law regression reveals a power law index of < 1.5 for all four planets. corroborating the absence of any significant systematic integration error we show in Fig. 1.

Fig. 3. Number of surviving planetesimals as a function of simulation time for the Saturn /Uranus zone. We see the first two of three phases we delineated in our Jupiter/Saturn study—the system appears to be in transition to the third phase at, the simulation's end.

Fig. 4. Particles were grouped according to initial semimajor axes in 0.2 AU intervals. and sorted with respect to their lifetimes. High and low values represent, the first and third quartiles, respectively. Jupiter and Saturn commensurabilities are indicated across the bottom. while those for Uranus and Neptune are indicated at the top. With the exception of the long-life band centered at 14.2 AU, we see that 75% of the planetesimals are eliminated in 10^7 years. We can also see long-life bands centered at 12.5 and 16 AU.

Fig. .5. Mean initial semimajor axis ±1 standard deviation of particles eliminated within each 5000 year period.

Fig. 6. Results taken from our Jupiter/Saturn study indicating the number of particles eliminated by both Jupiter and Saturn as a function of the initial particle semimajor axis. We have fit Gaussian functions through the data to more clearly indicate where each curve is peaked.

Fig. i'. The number of particles eliminated by both Saturn and Uranus as a function of the initial particle semimajor axis. As with Fig. 6, we fit Gaussian functions through the data to indicate more clearly where the results are peaked. We see a much greater splitting of the peaks than in the Jupiter/Saturn zone.

Fig. 8. Fraction of remaining particles as a function of time for inclinations 0°, 5°, 10°, 15°, and 20°. Each curve represents particles with initial inclinations ±0.5° of the aforementioned values (except for the zero-inclination curve that ranges from 0° to 0.5°, Here we see that the more highly inclined particles generally have longer lifetimes.

Fig. 9. Mean initial inclination ±1 standard deviation of particles eliminated within each .5000 year period. Consistent with Fig. 8, we see a general upwards trend, indicating that more highly inclined particles have generally longer lifetimes.

Fig. 10. Similar to Fig. 8, Fig. 10 is a "family of curves" indicating the fraction of particles remaining over time as a function of initial eccentricity. Curves are for eccentricity ranges O + 0.025, 0.05 ± 0.025, 0.10 ± 0.025, 0.15 ± 0.025, and 0.20 ± 0.025. Generally, highly eccentric particles are eliminated quickly, and we are increasingly left with a population of particles that began on more circular orbits. The lone possible exception is for the 0.05 curve that has a depletion rate very similar to that for the O eccentricity curve for the first 10^6 years.

Fig. 11. Mean initial eccentricities ±1 standard deviation of particles eliminated within each 5000-year period. Consistent with Fig. 10, we see a clear downwards trend, indicating that, as time passes, we are left with a population of particles that began the simulation on more nearly-circular orbits.

Fig. 12. The number of surviving planetesimals as a function of time and initial semimajor axis range. We see strong resonant effects have quickly depleted bands near 13 and 15 AU, while we see bands at 12.5, 14.4, 1.5,5. and 16 AU, in which particles are longer-lived.

Fig. 13. Plot of semimajor axis versus eccentricity for all 13.5 particles that survived the first 100 My of simulation time. We see three, perhaps four, long-life bands centered at 12..5.14.2. and 16 AU. Only one particle. from the 12..5 AU band, survived the entire 1 By integration.

Fig. 14. Number of surviving planetesimals as a function of simulation time for the Uranus/Neptune zone. Here we see a curve very similar to that from our Saturn/Uranus study.

Fig. 1.5. Similar to Figure 4, particles were grouped according to initial semimajor axis in 0.2 AU intervals. and sorted with respect to their lifetimes. High and low values represent the first and third quartiles. respectively. Jupiter and Saturn commensurabilities are indicated across the bottom, and those for Uranus and Neptune are indicated at the top. We see the long-life band at 26 AU. With the exception of particles near to the Uranus and Neptune 1:1 commensurabilities, 75% of the planetesimals are eliminated in 10^7 years.

Fig. 16. Mean initial semimajor axis ±1 standard deviation of particles eliminated within each

.5000 -year period.

Fig. 17. The number of particles eliminated by both Uranus and Neptune as a function of the initial particle semimajor axis. As with Figs. 6 and 7, we fit Gaussian functions through the results to indicate more clearly where they are pealied. We see more splitting of the pealis than in the Jupiter/Saturn zone, but less than Saturn/Uranus.

Fig. 18. Fraction of remaining particles as a function of time for inclinations of 0°, .5°, 10°, 15°. and 20°. Each curve represents particles with initial inclinations $\pm 0.5°$ of the aforementioned values (except for the zero-inclination curve which ranges from 0° to 0..5°. The zero-inclination curve has a sharply increased depletion rate for the first 5×10^5 years, with respect particles having more highly-inclined orbits. By 3×10^6 years, all surviving particles are either near to the invariable plane or very highly-inclined.

Fig. 19. Mean initial inclination $\pm$ 1 standard deviation of particles eliminated within each 5000 year period. Consistent with Fig. 7 for our Saturn/Uranus simulation, we see a clear upwards trend, indicating that more highly inclined particles have generally longer lifetimes.

Fig. 20. "Family of curves" indicating the fraction of particles remaining over time as a function of initial eccentricity. Curves are for the same eccentricity ranges as in Fig 8. Highly eccentric particles are eliminated quickly, and we are increasingly left with a population characterized by particles that began on more circular orbits,

Fig. 21. Mean initial eccentricities $\pm$ 1 standard deviation of particles eliminated within each 5000 year period. Despite the indication in Fig. 16 that the more eccentric particles are eliminated more quickly, we see no clear trend of this here.

Fig, 22. The number of surviving planetesimals as a function of time and initial semimajor axis range. We see a more symmetric winnowing and a suggestion that resonant effects are more evenly spaced in the Uranus/Neptune zone than for Saturn/Uranus. We see bands at 22.5, 24.5, 26 AU, in which particles are longer-lived.

Fig. 23 Plot of semimajor axis versus eccentricity for all particles that survived the first 100 My of simulation time on moderately circular orbits. We see long-life bands centered at 24.5 and 26 AU. We also see 4 Neptune librators survived 100 My, one of which survived 1 By.

Jupiter		Saturn		Uranus		Neptune	
AU	Res.	AU	Res.	AU	Res.	AU	Res.
9.6	2:5	9.5	1:1	10.5	5:2	10.3	5:1
10.0	3:8	10.8	5:6	11.0	7:3	11.9	4:1
10.8	1:3	11.1	4:5	12.1	2:1	13.0	7:2
12.0	2:7	11.6	3:4	13.3	7:4	14.4	3:1
13. I	1:4	12.5	2:3	13.7	5:3	16,3	5:2
14.2	2:9	13.4	3:5	14.7	3:2	17.1	7:3
15.2	1:5	13.8	4:7	15.9	4:3	18.9	2:1
17.2	1:6	15.1	1:2	16.6	5:4		
		16.4	4:9	17.1	6:5		
		16.8	3:7	19.3	1:1		
		17.6	2:5				

Table 1

Distance	Alive	Jupiter	Saturn	Uranus	Neptune	Eject
9.0	0	0	3	0	0	0
9.2	0	0	0	0	0	0
9.4	0	0	2	0	0	0
9.6	0	0	8	0	0	0
9.8	0	0	13	0	0	0
10.0	0	0	19	0	0	0
10.2	0	0	21	0	0	0
10.4	0	1	20	5	0	0
10.6	0	0	31	1	1	0
10.8	0	0	44	5	0	0
11.0	0	1	57	5	0	0
11.2	0	1	71	19	2	0
11.4	0	0	71	14	0	0
11.6	0	1	112	20	1	0
11.8	0	0	118	39	0	0
12.0	0	0	137	40	5	0
12.2	0	1	156	46	2	0
12.4	1	4	226	51	4	0
12.6	0	2	233	51	6	1
12.8	0	0	222	75	5	0
13.0	0	3	252	115	1	0
13.2	0	2	250	132	7	0
13.4	0	1	255	164	8	0
13.6	0	0	275	172	12	0
13.8	0	2	283	210	6	0
14.0	0	1	260	242	10	0
14.2	0	1	230	264	8	0
14.4	0	4	222	259	10	0
14.6	0	2	175	285	15	0
14.8	0	0	57	412	0	0
15.0	0	0	30	373	3	0
15.2	0	1	21	377	0	0
15.4	0	0	26	346	4	0
15.6	0	0	22	313	2	0
15.8	0	0	24	291	2	0
16.0	0	0	12	276	2	0
16.2	0	0	9	239	2	0
16.4	0	0	9	205	2	0
16.6	0	0	2	173	0	0
16.8	0	0	6	142	1	0
17.0	0	0	0	112	1	0
17.2	0	0	4	104	1	0
17.4	0	0	4	57	0	0
17.6	0	0	0	64	0	0
17.8	0	0	2	46	0	0
18.0	0	0	2	45	0	0
18.2	0	0	0	14	0	0
18.4	0	0	0	20	0	0
18.6	0	0	0	7	0	0
18.8	0	0	0	6	0	0
19.0	0	0	0	9	0	0
19.2	0	0	0	5	0	0
19.4	0	0	0	1	0	0
Totals	1	28	3,996	5,851	123	1

Table 2

Planet	Planetary Distance (AU)	Planetesimal Mean		Planetesimal Std. Dev.	
		Initial	Final	Initial	Final
Jupiter	5.20	13.24	11.30	1.19	5.28
Saturn	9.54	13.25	13.37	1.21	3.47
Uranus	19.18	15.14	16.08	1.38	1.44
Neptune	30.06	14.00	22,11	1.23	2.61

Table 3

Inner	Number	Outer
0 ≤ a	3	a < 5.2
5.2 ≤ a	227	a < 9.5
9.5 ≤ a	9,295	a < 19.2
19.2 ≤ a	457	a < 30.1
30.1 ≤ a	12	a < 40.0
40.0 ≤ a	3	a < 50.0
50.0 ≤ a	0	a < 60.0
60.0 ≤ a	0	0< 70.0
70.0 ≤ a	1	a < 80.0
80.0 ≤ a	0	a < 90.0
90.0 ≤ a	1	a < 100.0
100.0 ≤ a	0	a < 200.0
200.0 ≤ a	0	
	1 ejection	

Table 4

Inclination	Alive	Jupiter	Saturn	Uranus	Neptune	Eject
0 ≤ i < 1	1	0	310	500	12	0
1 ≤ i < 2	0	2	258	479	10	0
2 ≤ i < 3	0	1	301	488	12	0
3 ≤ i < 4	0	9	321	444	7	0
4 ≤ i < 5	0	2	256	446	7	0
5 ≤ i < 6	0	2	273	439	11	0
6 ≤ i < 7	0	1	249	378	12	0
7 ≤ i < 8	0	1	254	346	8	0
8 ≤ i < 9	0	2	235	302	8	0
9 ≤ i < 10	0	1	226	292	5	0
10 ≤ i < 11	0	0	186	239	12	0
11 ≤ i < 12	0	1	168	232	2	0
12 ≤ i < 13	0	1	148	179	3	0
13 ≤ i < 14	0	1	130	180	7	0
14 ≤ i < 15	0	3	105	179	2	0
15 ≤ i < 16	0	0	89	139	1	0
16 ≤ i < 17	0	0	88	106	2	0
17 ≤ i < 18	0	0	83	107	1	0
18 ≤ i < 19	0	0	57	65	1	0
19 ≤ i < 20	0	0	54	68	0	0
20 ≤ i < 21	0	0	36	50	0	1
21 ≤ i < 22	0	1	29	45	0	0
22 ≤ i < 23	0	0	28	42	0	0
23 ≤ i < 24	0	0	23	28	0	0
24 ≤ i < 25	0	0	27	16	0	0
25 ≤ i < 26	0	0	15	18	0	0
26 ≤ i < 27	0	0	14	12	0	0
27 ≤ i < 28	0	0	9	6	0	0
28 ≤ i <29	0	0	7	4	0	0
29 ≤ i < 30	o	0	8	5	0	0
Totals	1	28	3,987	5,834	123	1

Table 5

Jupiter		Saturn		Uranus		Neptune	
A U	Res.	A U	Res.	AU	Res.	A U	Res.
19.0	1:7	19.8	1:3	19.2	1:1	19.0	2:1
20.8	1:8	22.0	2:7	21.3	6:7	20.7	7:4
22.5	1:9	24.0	1:4	21.8	5:6	21.4	5:3
		26.0	2:9	22.3	4:5	23.0	3:2
		27.9	1:5	23.3	3:4	24.0	7:5
				24.1	5:7	24.8	4:3
				25.3	2:3	25.9	5:4
				26.2	5:8	27.1	7:6
				27.1	3:5	30.1	1:1
				2 8 . 0	4:7		
				28,4	5:9		
				30.6	1:2		

Table 6

Distance	Alive	Jupiter	Saturn	Uranus	Neptune	Eject
1s.0	o	0	0	0	0	0
18.2	0	0	0	0	0	0
18.4	0	0	0	0	0	0
18.6	0	0	0	1	0	0
18.8	0	0	0	0	0	0
19.0	0	0	0	2	0	0
19.2	0	0	0	7	0	0
19.4	0	0	0	8	0	0
19.6	0	0	0	23	0	0
19.8	0	0	0	15	0	0
20.0	0	0	0	19	0	0
20.2	0	0	0	30	0	0
20.4	0	0	0	33	0	0
20.6	0	0	0	37	2	0
20.8	0	0	0	54	4	0
21.0	0	0	0	67	4	0
21.2	0	0	1	69	6	0
21.4	0	0	1		15	0
21.6	0	0	0	1::	22	0
21.8	0	0	0	119	24	0
22.0	0	0	1	134	41	0
22.2	0	0	0	140	38	0
22.4	0	0	0	161	47	0
22.6	0	0	3	174	59	0
22.8	0	0	0	178	67	0
23.0	0	0	2	231	60	0
23.2	0	0	0	225	87	0
23.4	0	0	1	196	157	0
23.6	0	0	0	219	159	0
23.8	0	0	0	196	219	0
24.0	0	0	0	199	202	0
24.2	0	0	1	182	264	0
24.4	0	1	1	175	254	0
24.6	0	0	0	148	290	0
24.8	0	0	0	160	276	0
25.0	0	0	0	140	274	0
25.2	0	0	0	119	266	0
25.4	0	0	1	115	257	0
25.6	0	0	0	90	236	0
25.8	0	0	0	91	243	1
26.0	0	1	0	89	229	0
26.2	0	0	0	74	245	1
26.4	0	0	0	64	203	0
26.6	0	0	2	45	191	0
26.8	0	0	0	38	188	0
27.0	0	0	0	28	179	0
27.2	0	0	0	22	141	0
27.4	0	0	2	18	137	0
27.6	0	0	0	14	112	0
27.8	0	0	0	3	80	0
28.0	0	0	0	9	72	0
28.2	0	0	0	5	47	0
28.4	0	0	0	4	51	0
28.6	0	0	0	4	46	0
28.8	0	0	0	1	29	0
29.0	0	0	0	0	27	0
29.2	0	0	0	0	16	0
29.4	0	0	0	0	21	0
29.6	0	0	0	0	7	0
29.8	1	0	0	0	6	0
30.0	0	0	0	0	6	0
30.2	0	0	0	0	5	0
30.4	0	0	0	0	3	0
30.6	0	0	0	0	1	0
Totals	1	2	16	4,364	5.615	2

Table 7

Planet	Planetary Distance (AU)	Planetesimal Mean		Planetesimal Std. Dev.	
		Initial	Final	Initial	Final
Jupiter	5.20	25.25	24.16	1.20	22.50
Saturn	9.54	24.11	26.00	2.11	6.70
Uranus	19.18	23.70	23.11	1.67	2.14
Neptune	30.06	25.46	26.68	1.60	2.20

Table 8

Inner	Number	Outer
0 ≤ a	o	a < 5.2
5.2 ≤ a	1 .	a < 9.5
9.5 ≤ a	142	a < 19.2
19.2 ≤ a	9,479	a< 30.1
30.1 ≤ a	360	a < 40.0
40.0 ≤ a	4	a < 50.0
50.0 ≤ a	3	a <60.0
60.0 ≤ a	0	a <70.0
70.0 ≤ a	0	a < 80.0
80.0 ≤ a	0	a <90.0
90.0 ≤ a	0	a <100.0
100.0 ≤ a	0	a <200.0
200.0 ≤ a	0	
	11 ejections	

Table 9

Inclination	Alive	Jupiter	Saturn	Uranus	Neptune	Eject
$0 \leq i < 1$	0	0	1	350	471	2
$1 \leq i < 2$	0	0	2	308	471	0
$2 \leq i < 3$	0	0	0	336	452	0
$3 \leq i < 4$	0	0	2	330	457	0
$4 \leq i < 5$	0	0	2	282	409	0
$5 \leq i < 6$	0	0	1	309	408	0
$6 \leq i < 7$	0	0	2	276	354	0
$7 \leq i < 8$	0	1	2	282	344	0
$8 \leq i < 9$	0		0	257	291	
$9 \leq i < 10$	0	0	0	234	277	
$10 \leq i < 11$	0	0	0	199	251	0
$11 \leq i < 12$	0	0	0	182	237	0
$12 \leq i < 13$	0	0	0	147	163	0
$13 \leq i < 14$	0	0	0	153	173	0
$14 \leq i < 15$	0	0	2	115	150	0
$15 \leq i < 16$	0	0	1	131	121	0
$16 \leq i < 17$	0	0	0	74	122	0
$17 \leq i < 18$	0	0	0	80	94	0
$18 \leq i < 19$	0	-	0	54	72	0
$19 \leq i < 20$		0	0	53	66	0
$20 \leq i < 21$		0	0	41	53	0
$21 \leq i < 22$	0	0	1	33	37	0
$22 \leq i < 23$	0	0	0	31	39	0
$23 \leq i < 24$	0	0	0	25	26	0
$24 \leq i < 25$	0	0	0	20	24	0
$25 \leq i < 26$	0	0	0	15	16	0
$26 \leq i < 27$	0	0	0	11	8	0
$27 \leq i < 28$	0	0	0	12	6	0
$28 \leq i < 29$	0	0	0	6	5	0
$29 \leq i < 30$	0	0	0	5	6	0
Totals	1	2	16	4,351	5,603	2

Table 10

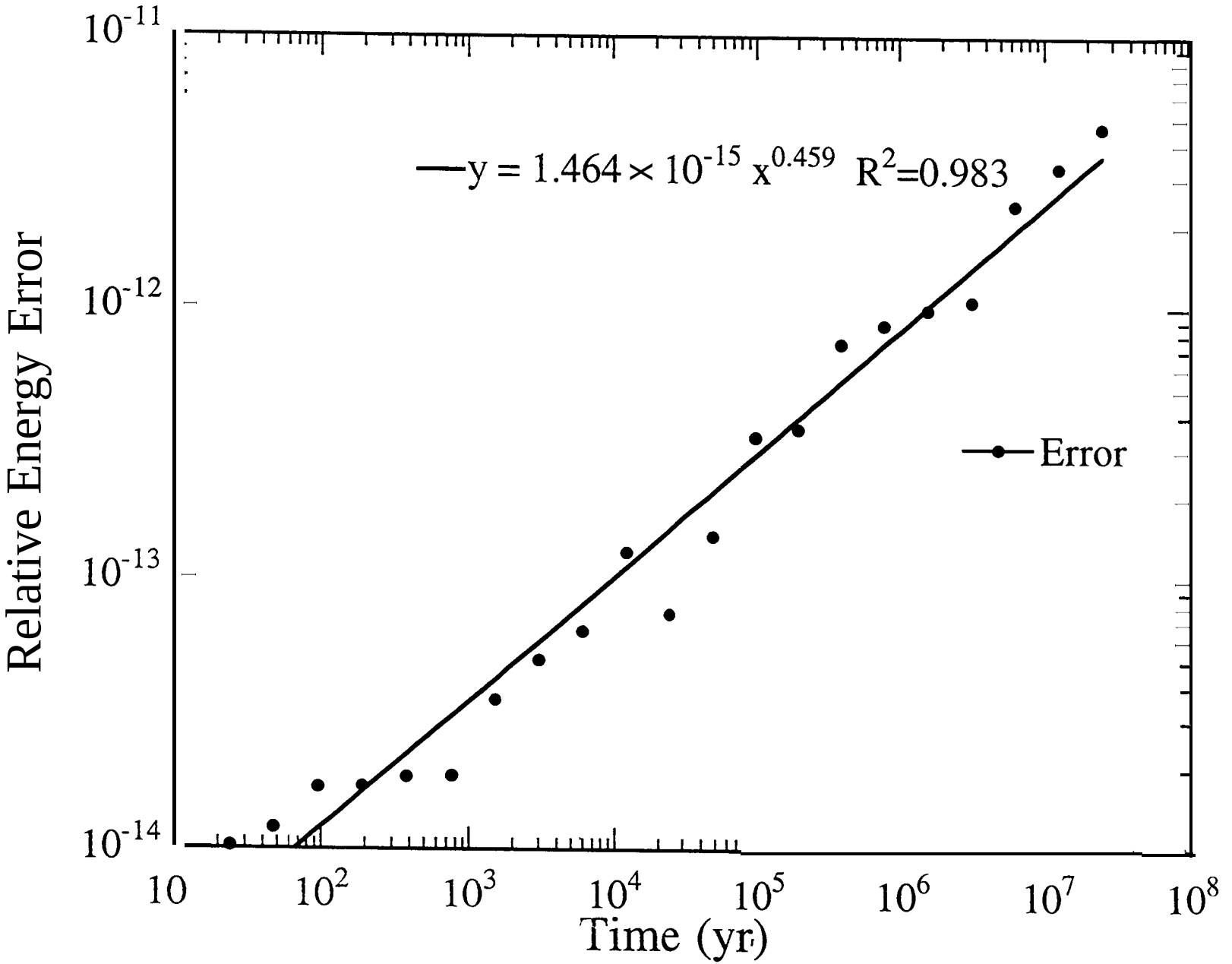
Relative Energy Error
10^{-11}
10^{-12}
10^{-13}
10^{-14}
—y = 1.464 × 10^{-15} $x^{0.459}$ R^2=0.983
Error
10
10^2
10^3
10^4
10^5
10^6
10^7
10^8
Time (yr)

Figure 1

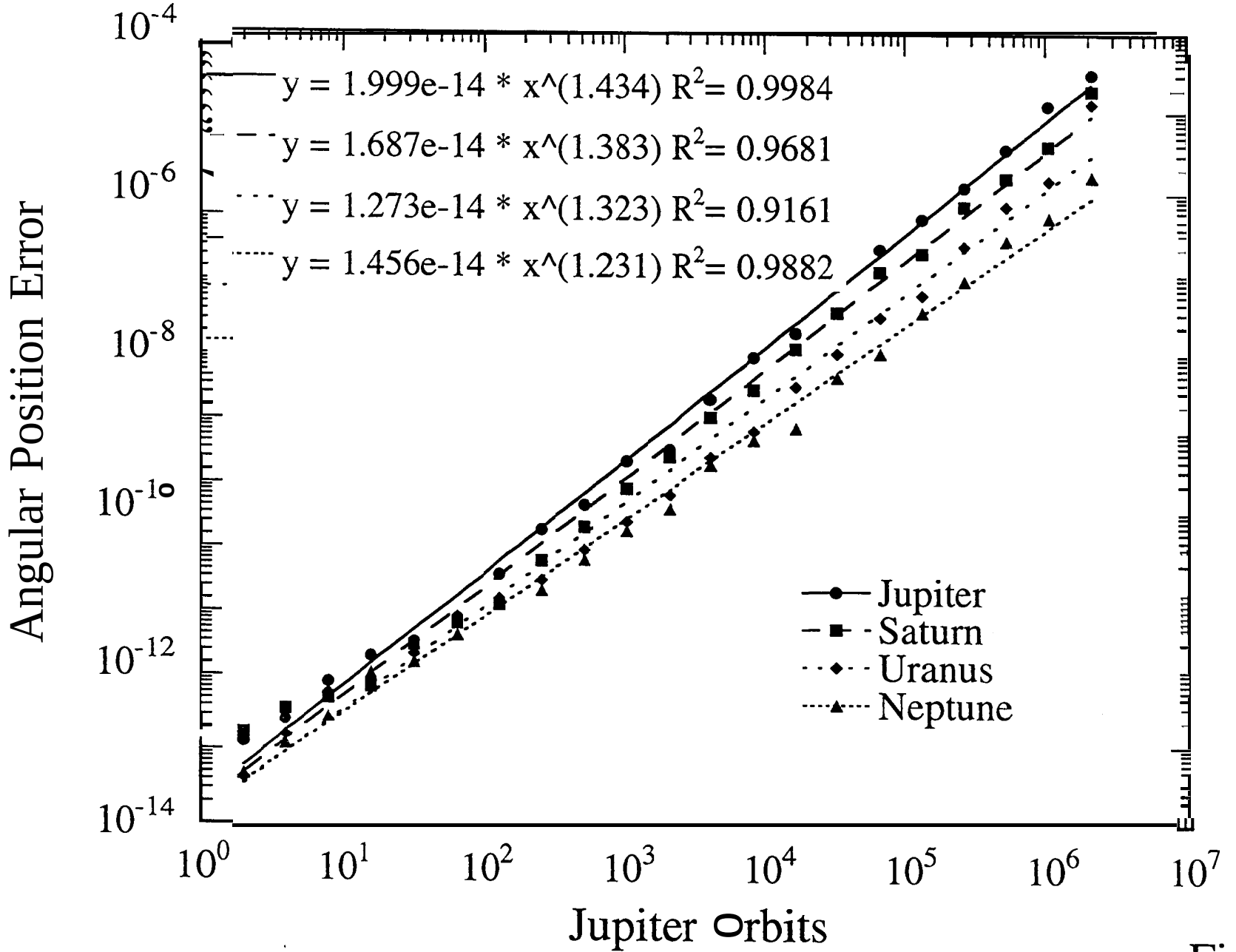
y = 1.999e-14 * x^(1.434) R2= 0.9984
y = 1.687e-14 * x^(1.383) R2= 0.9681
y = 1.273e-14 * x^(1.323) R2= 0.9161
y = 1.456e-14 * x^(1.231) R2= 0.9882
Jupiter
Saturn
Uranus
Neptune
Angular Position Error
Jupiter Orbits
10-4
10-6
10-8
10-10
10-12
10-14
100
101
102
103
104
105
106
107

Figure 2

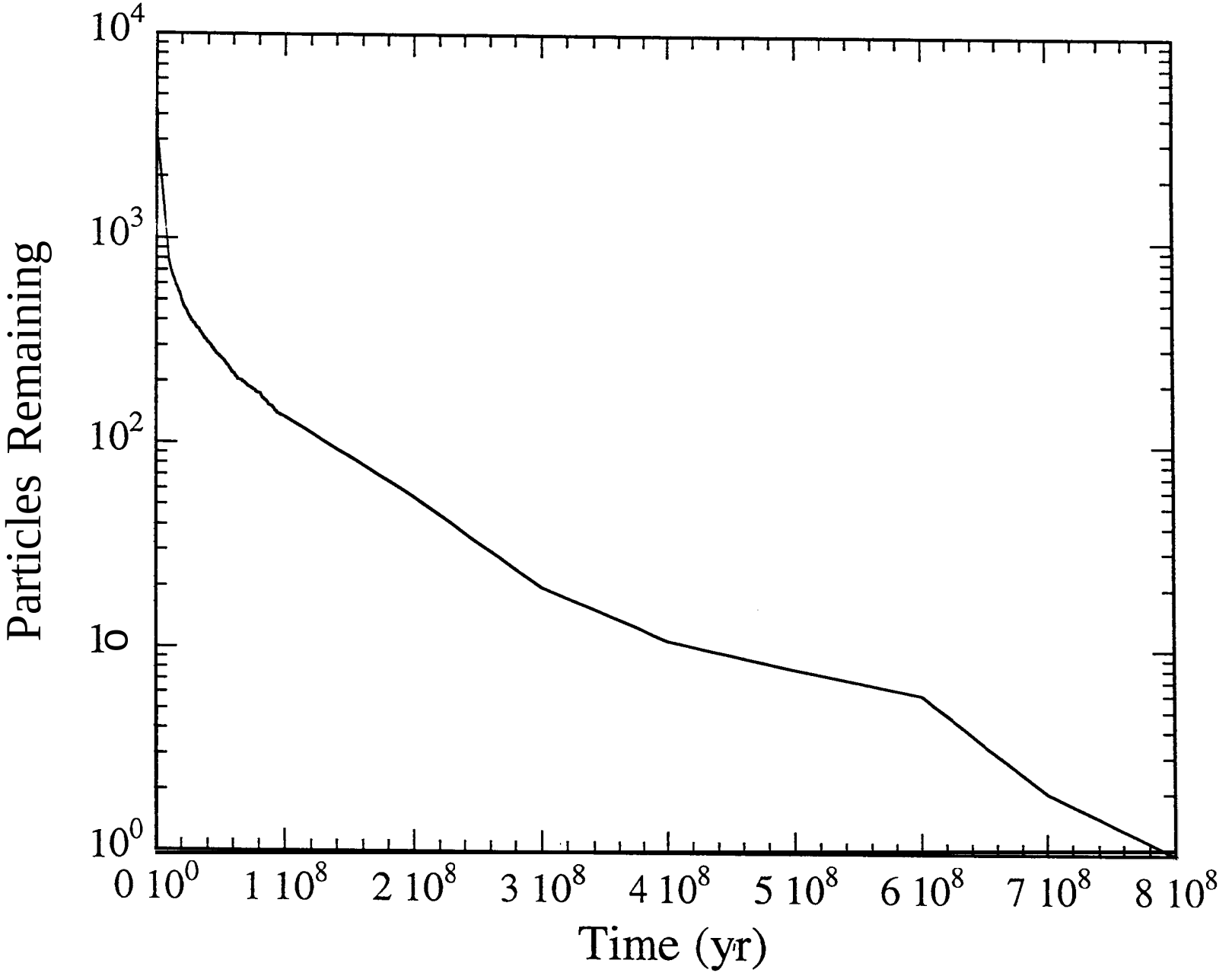
Particles Remaining
10^4
10^3
10^2
10
10^0
0 10^0
1 10^8
2 10^8
3 10^8
4 10^8
5 10^8
6 10^8
7 10^8
8 10^8
Time (yr)

Figure 3

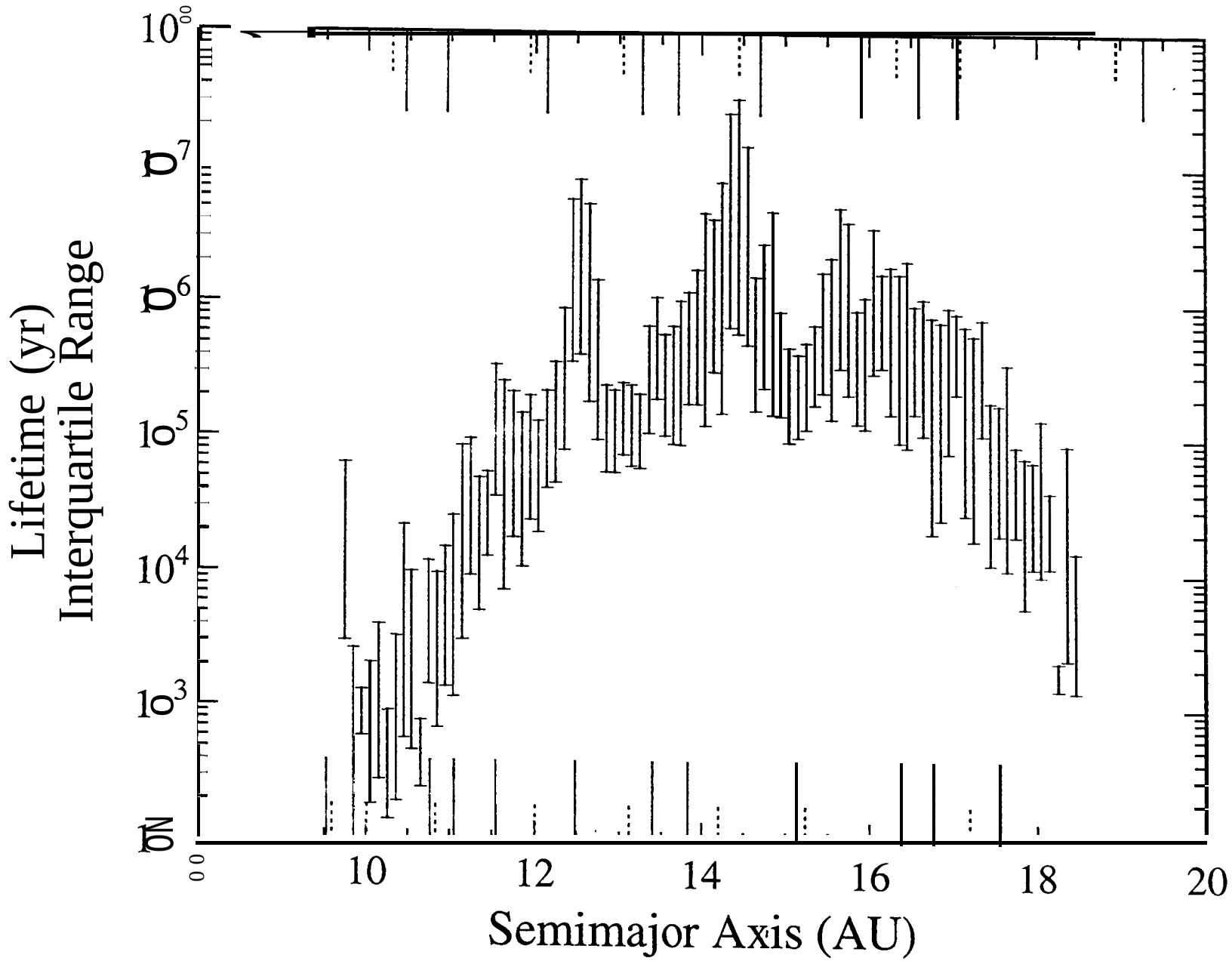
Lifetime (yr)
Interquartile Range
Semimajor Axis (AU)
10
12
14
16
18
20

Figure 4

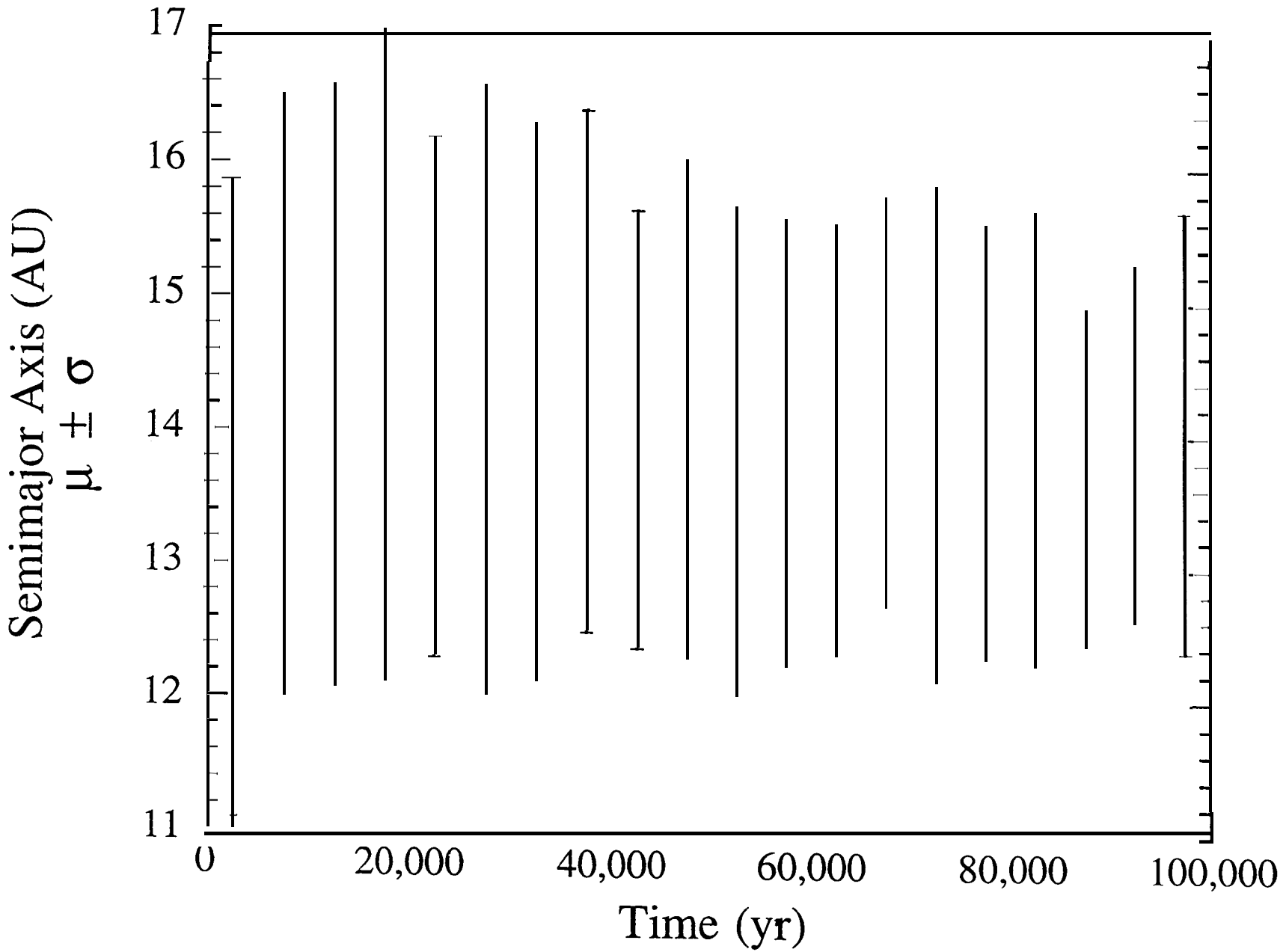
Semimajor Axis (AU)
μ ± σ
17
16
15
14
13
12
11
0
20,000
40,000
60,000
80,000
100,000
Time (yr)

Figure 5

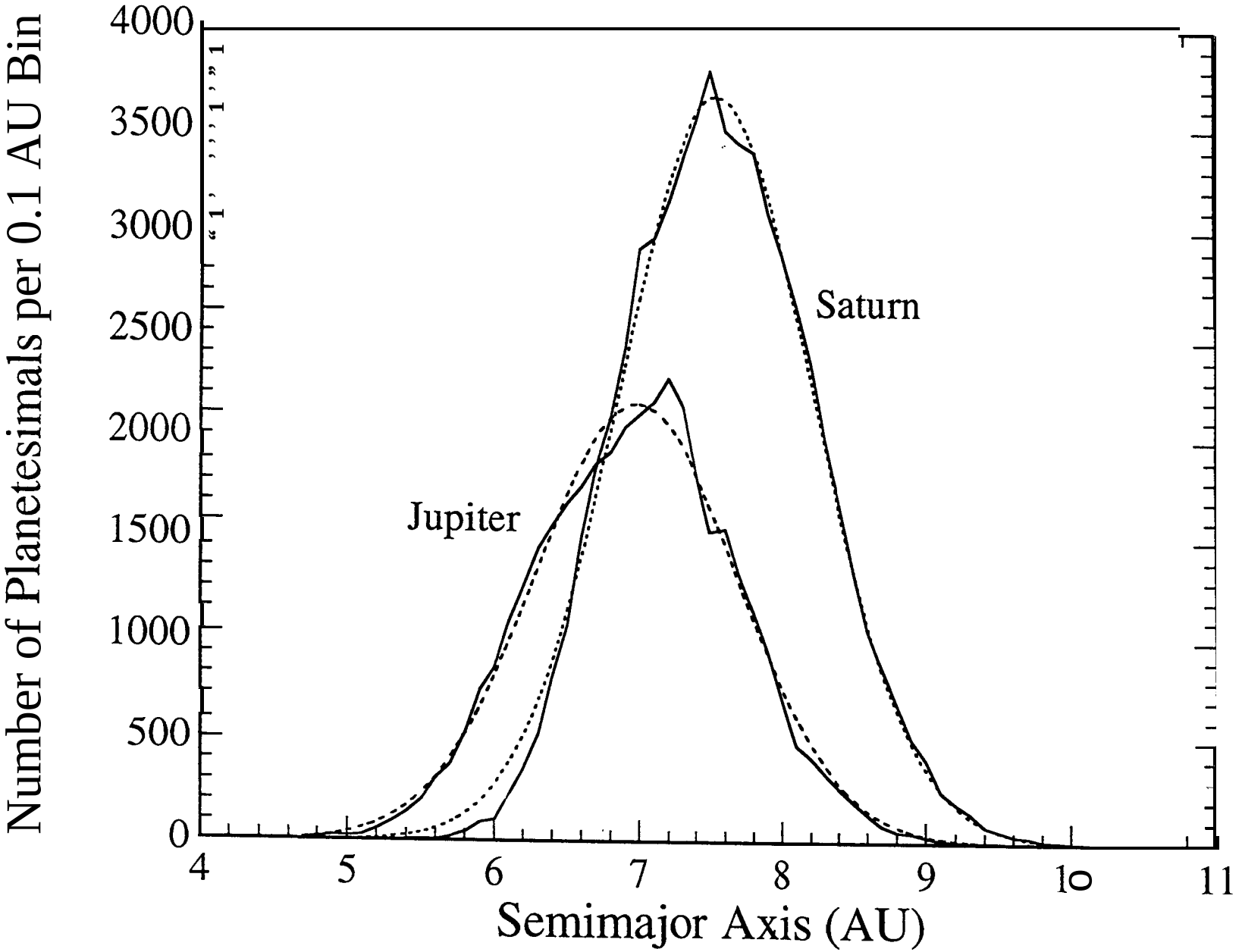
Number of Planetesimals per 0.1 AU Bin
4000
3500
3000
2500
2000
1500
1000
500
0
4
5
6
7
8
9
10
11
Semimajor Axis (AU)
Saturn
Jupiter

Figure 6

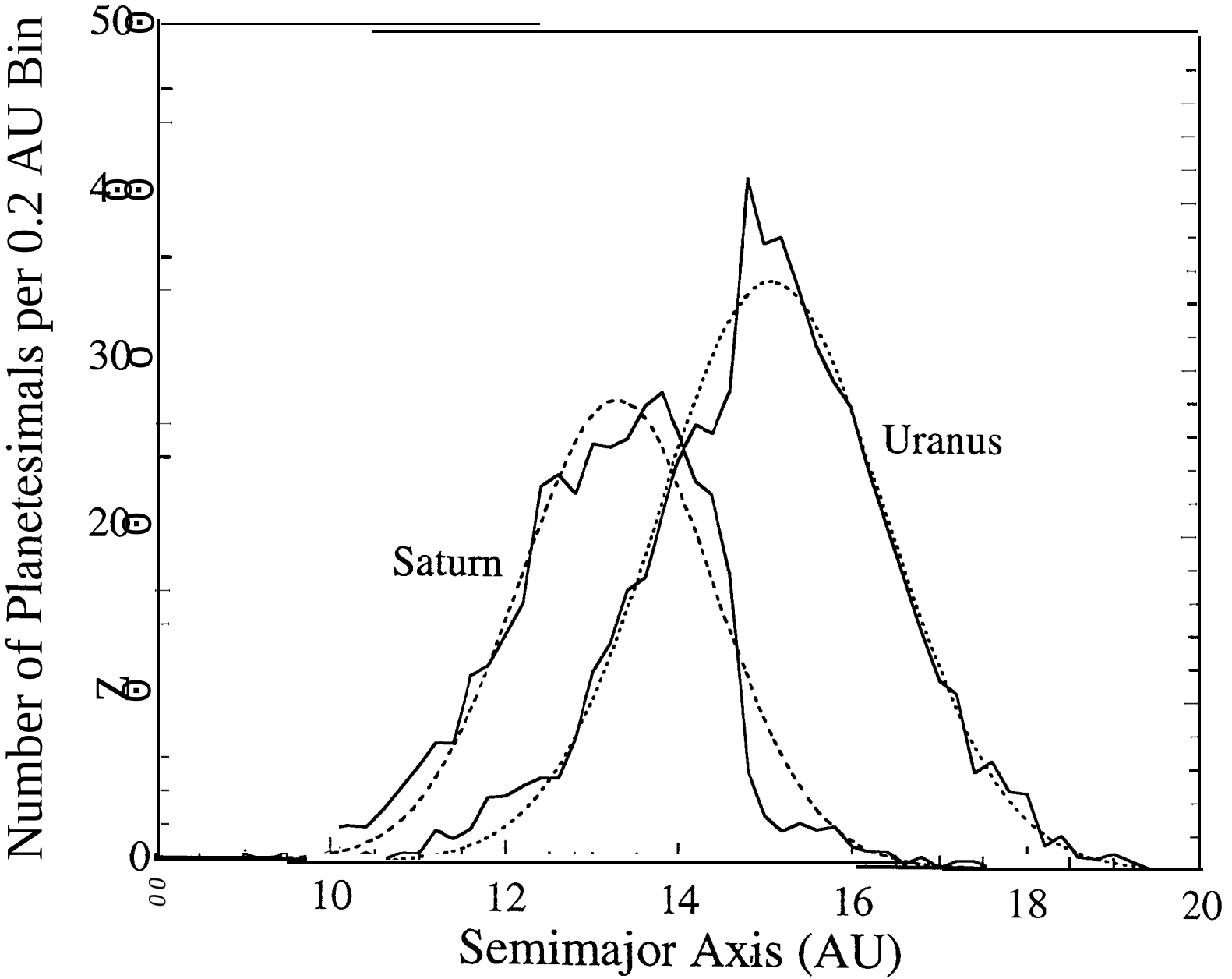
Number of Planetesimals per 0.2 AU Bin
0
10
20
30
40
50
10
12
14
16
18
20
Semimajor Axis (AU)
Saturn
Uranus

Figure 7

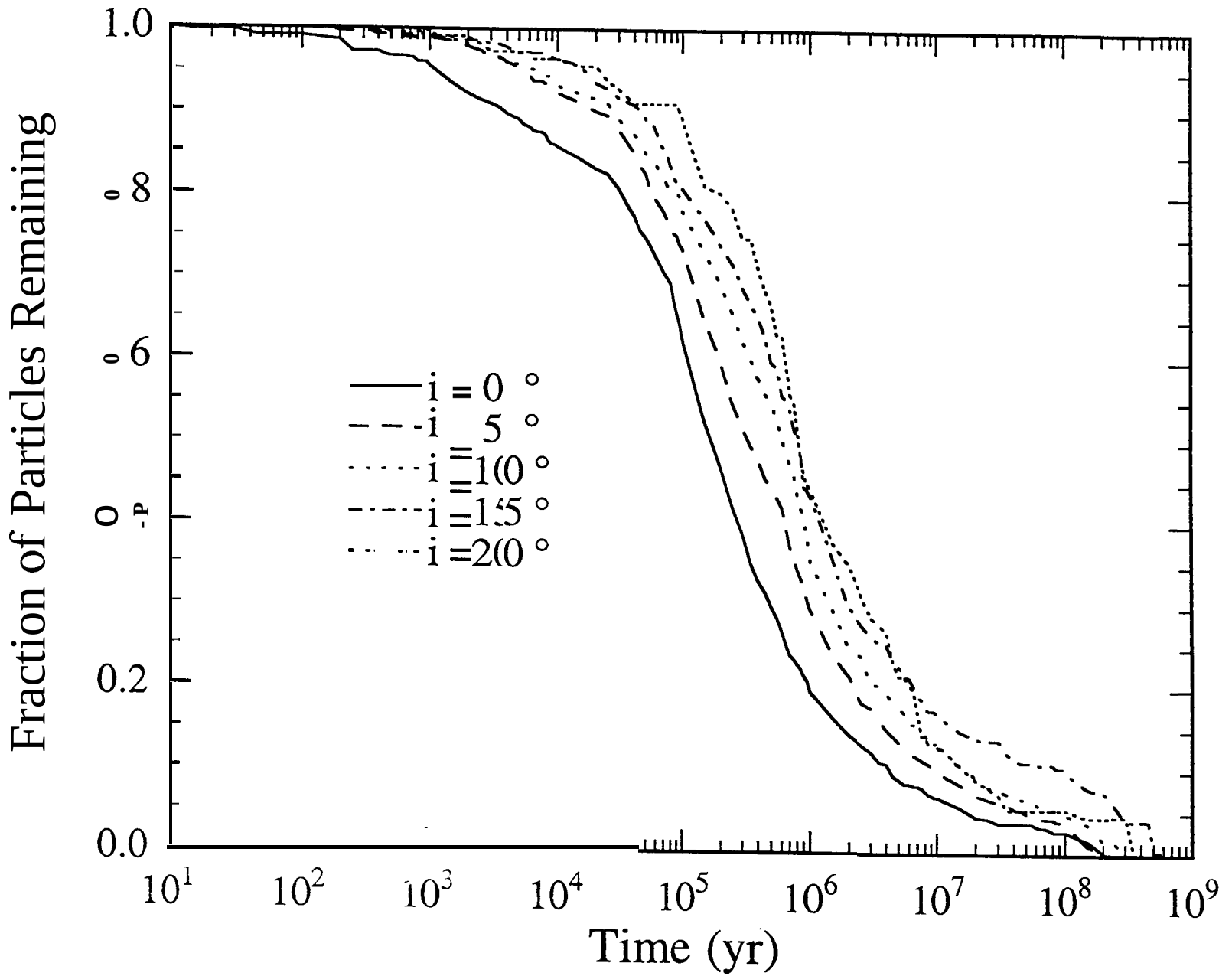
1.0
0.8
0.6
0.4
0.2
0.0
Fraction of Particles Remaining
i = 0 °
i = 5 °
i =10 °
i =15 °
i =20 °
10^1
10^2
10^3
10^4
10^5
10^6
10^7
10^8
10^9
Time (yr)

Figure 8

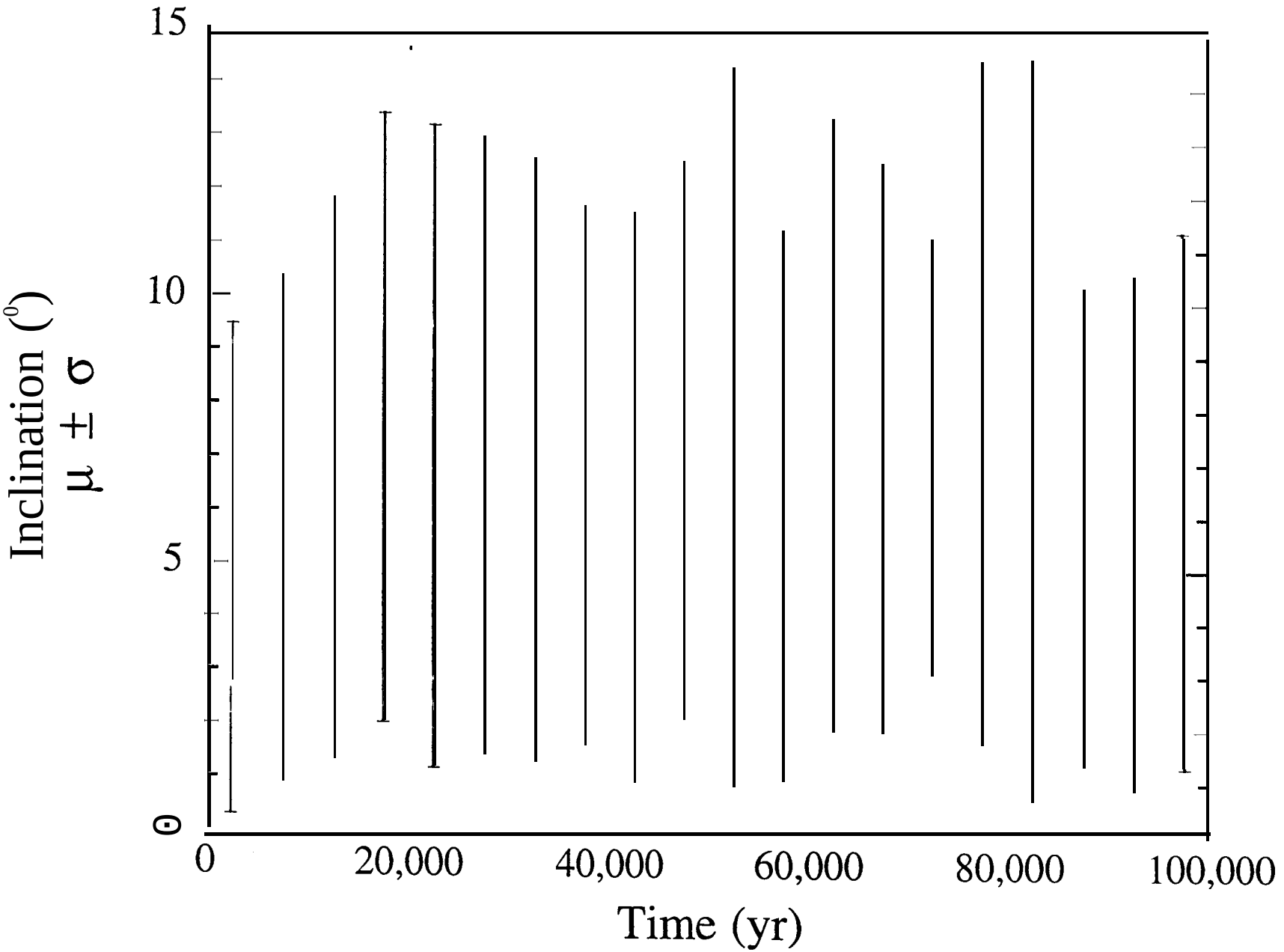
15
10
5
0
Inclination (°)
μ ± σ
0
20,000
40,000
60,000
80,000
100,000
Time (yr)

Figure 9

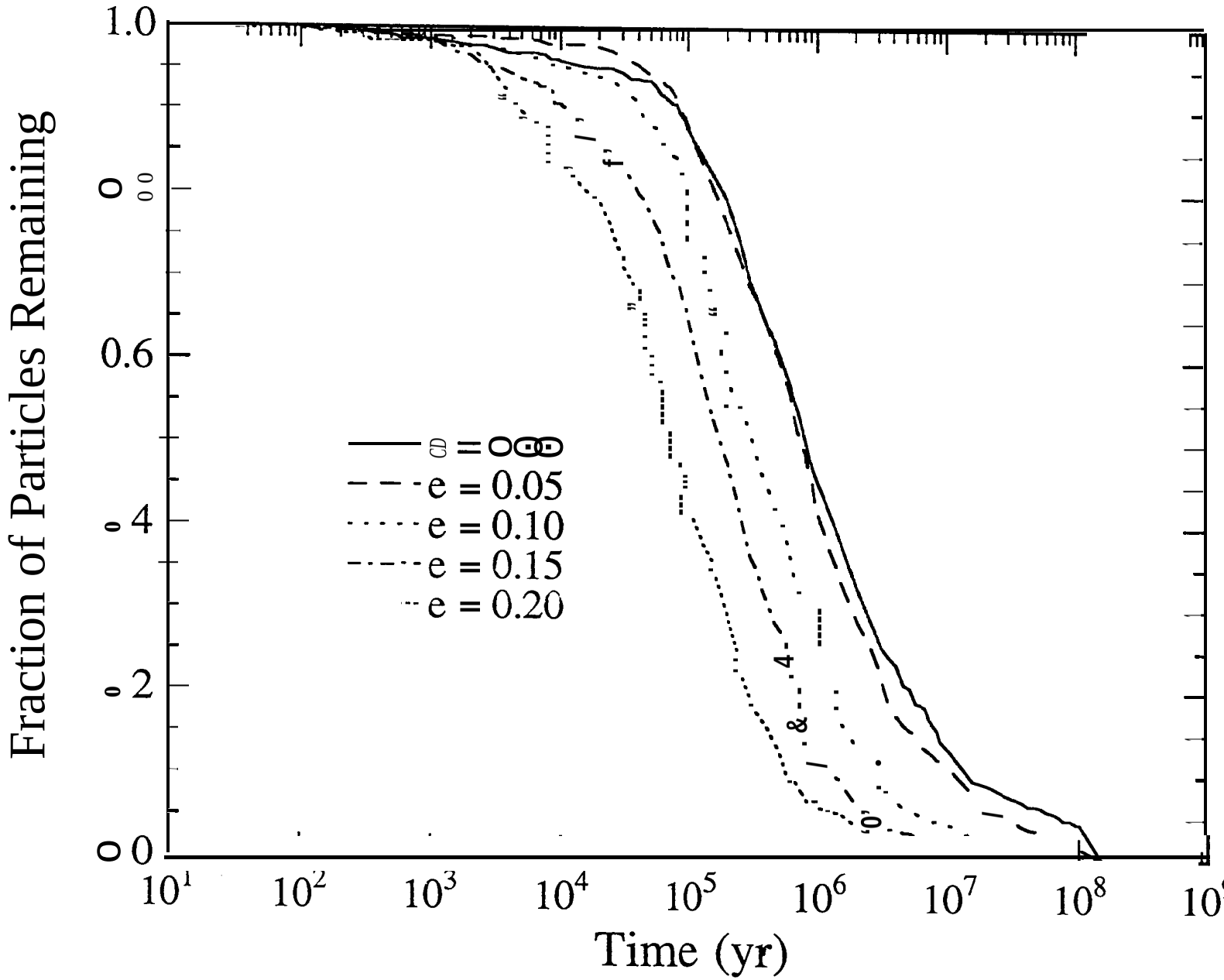
Fraction of Particles Remaining
1.0
0.6
0 0
10^1
10^2
10^3
10^4
10^5
10^6
10^7
10^8
10^9
Time (yr)
e = 0.05
e = 0.10
e = 0.15
e = 0.20

Figure 10

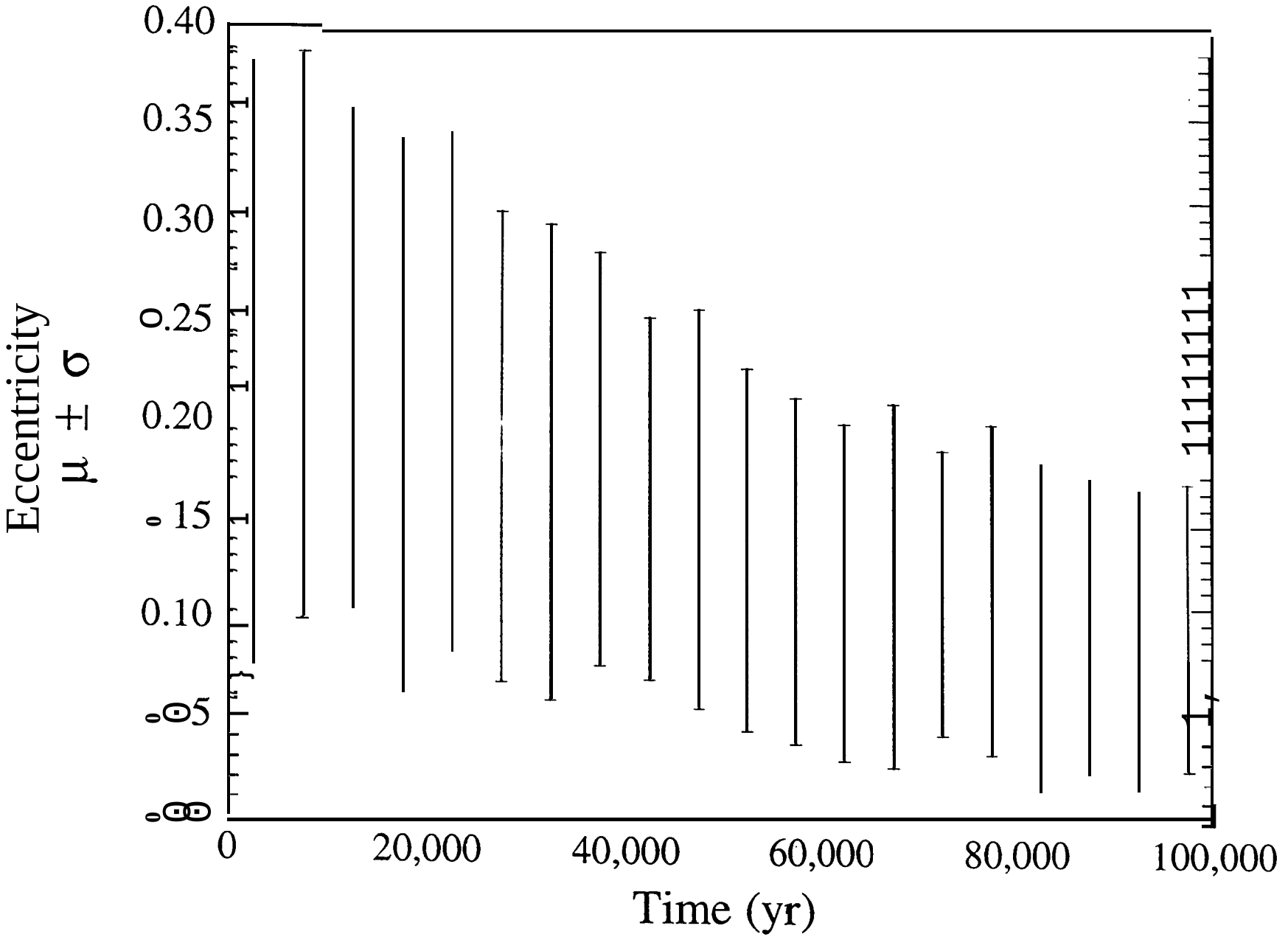
Eccentricity
μ ± σ
0.40
0.35
0.30
0.25
0.20
0.15
0.10
0.05
0.00
0
20,000
40,000
60,000
80,000
100,000
Time (yr)

Figure 11

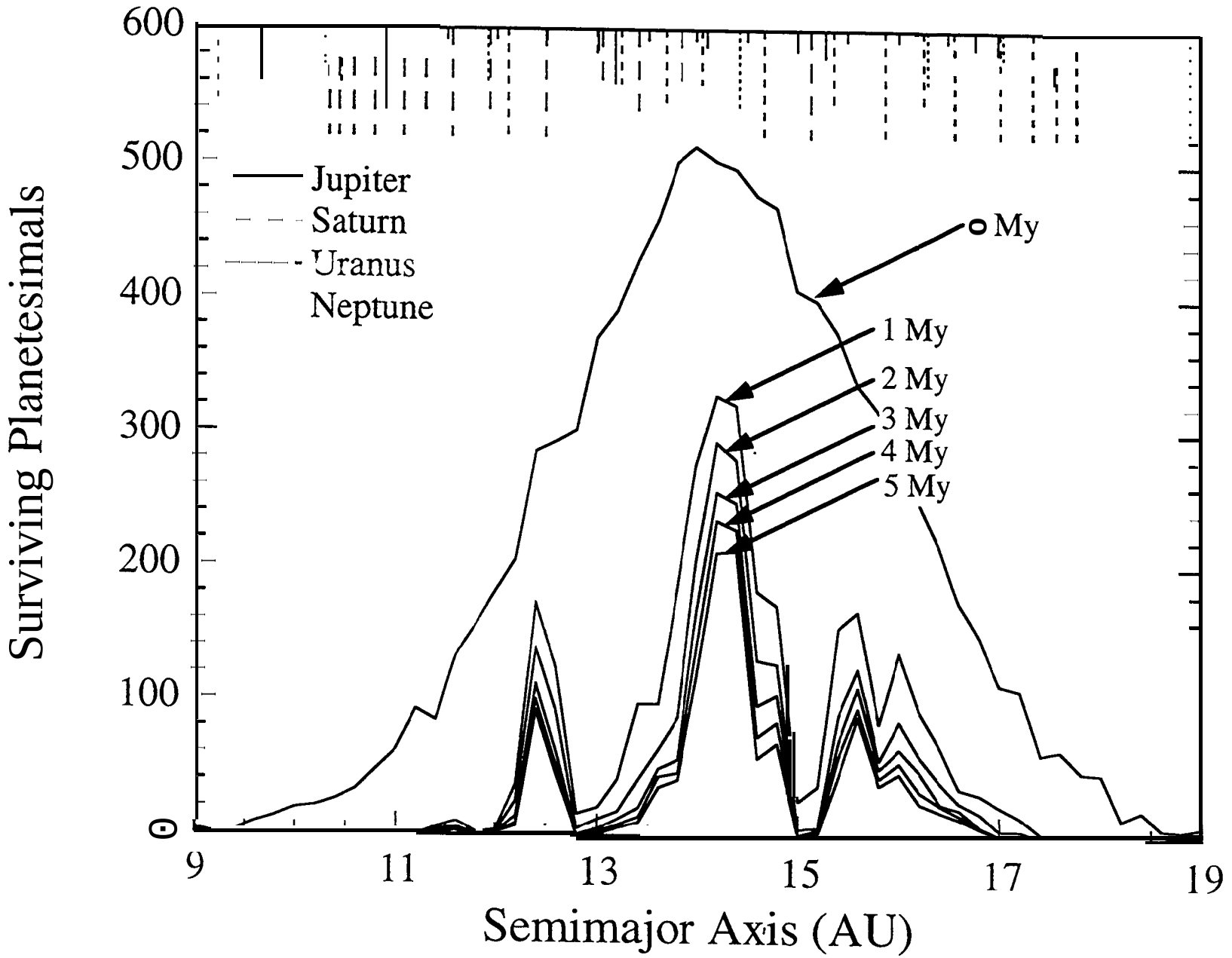
Surviving Planetesimals
600
500
400
300
200
100
0
Jupiter
Saturn
Uranus
Neptune
0 My
1 My
2 My
3 My
4 My
5 My
9
11
13
15
17
19
Semimajor Axis (AU)

Figure 12

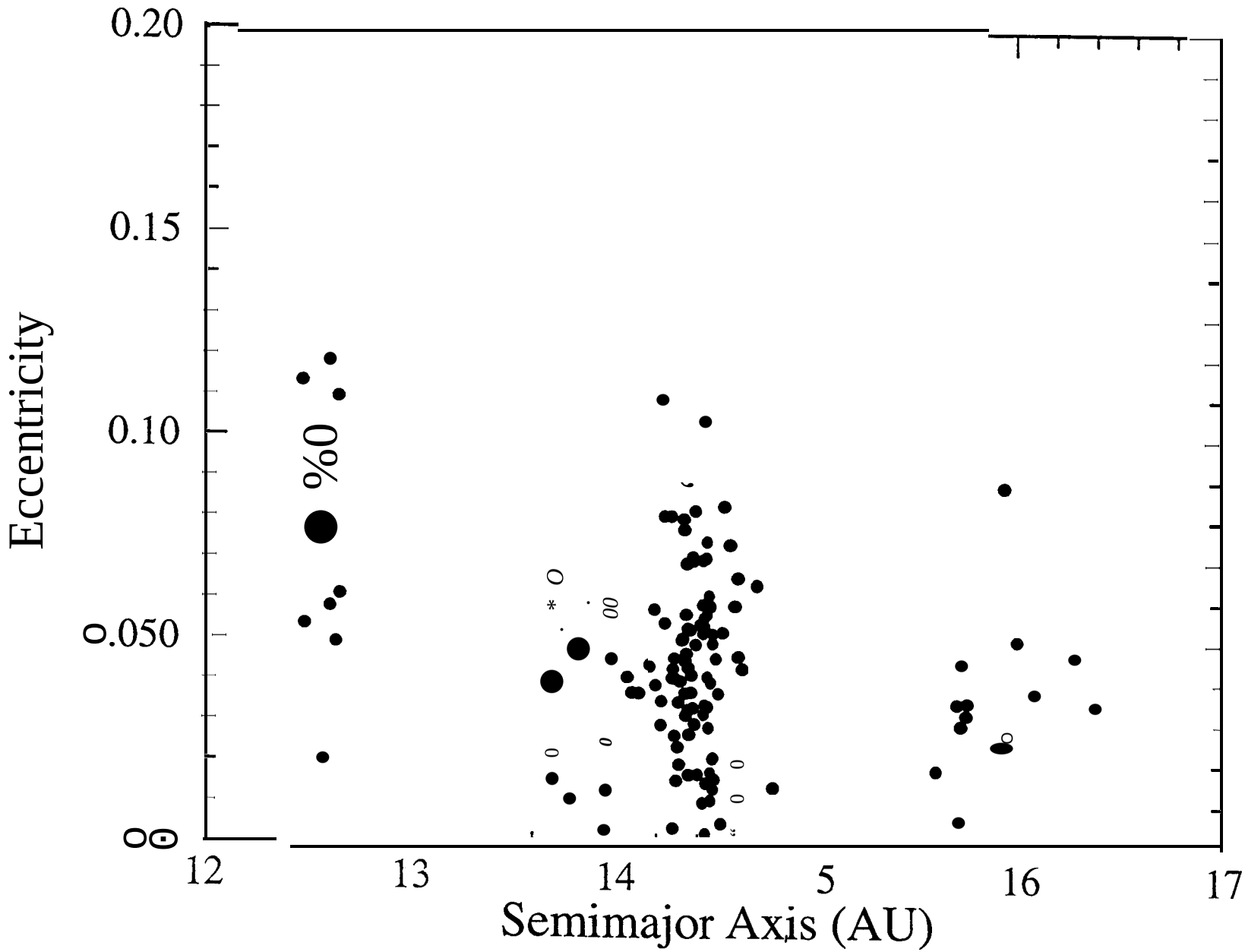
0.20
0.15
0.10
0.050
0
Eccentricity
12
13
14
5
16
17
Semimajor Axis (AU)

Figure 13

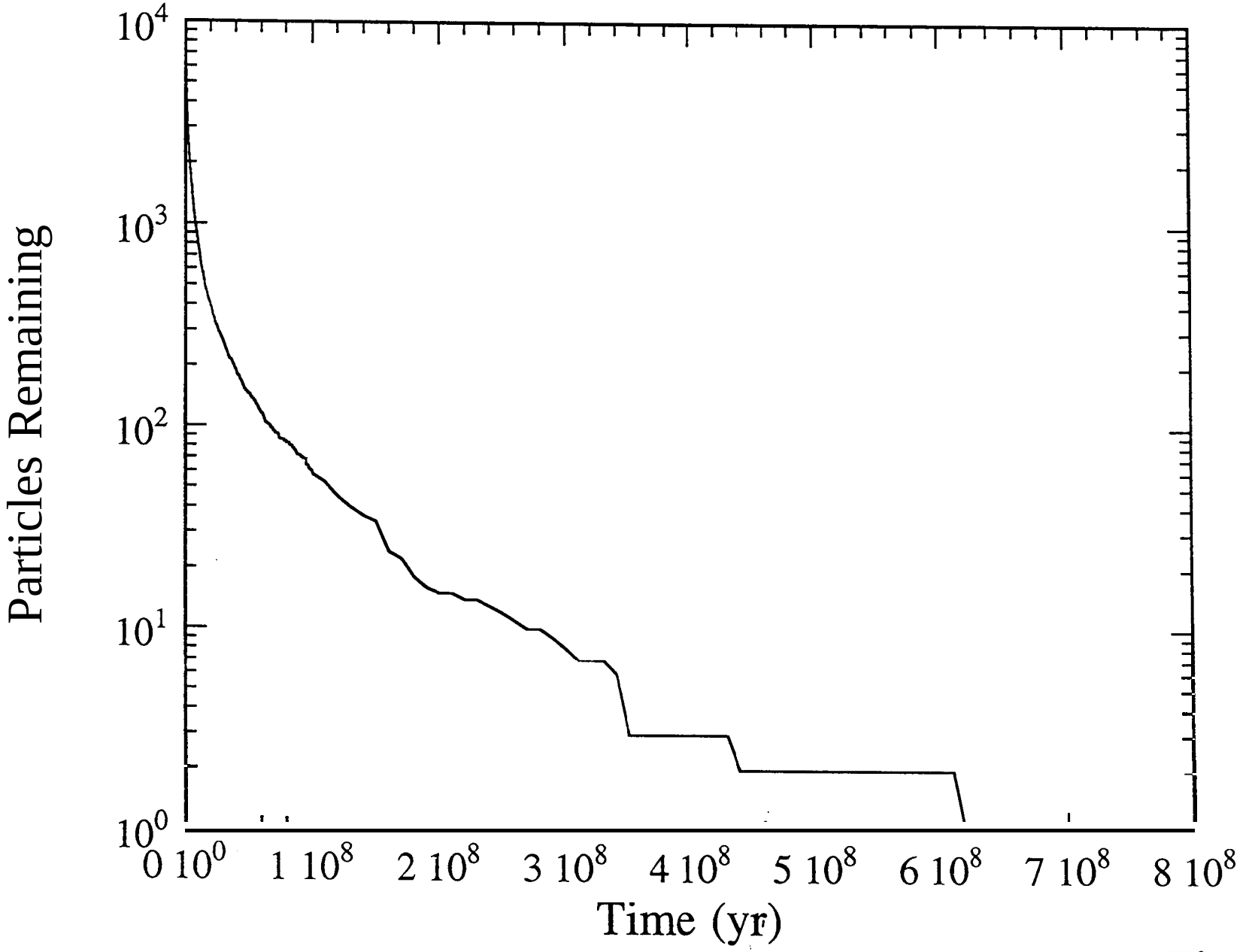
Particles Remaining
10^4
10^3
10^2
10^1
10^0
0 10^0
1 10^8
2 10^8
3 10^8
4 10^8
5 10^8
6 10^8
7 10^8
8 10^8
Time (yr)

Figure 14

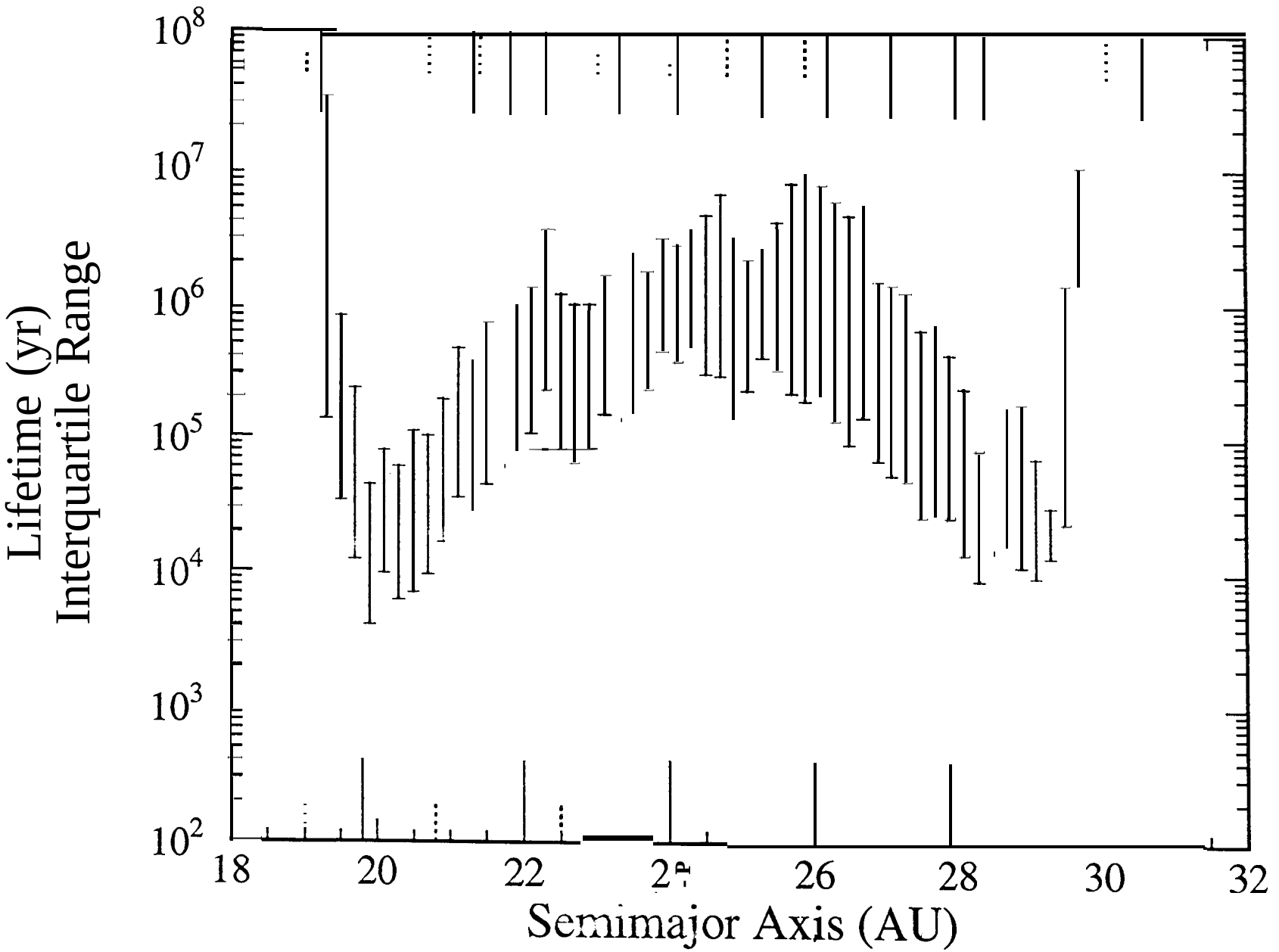
Lifetime (yr)
Interquartile Range
10^8
10^7
10^6
10^5
10^4
10^3
10^2
18
20
22
24
26
28
30
32
Semimajor Axis (AU)

Figure 15

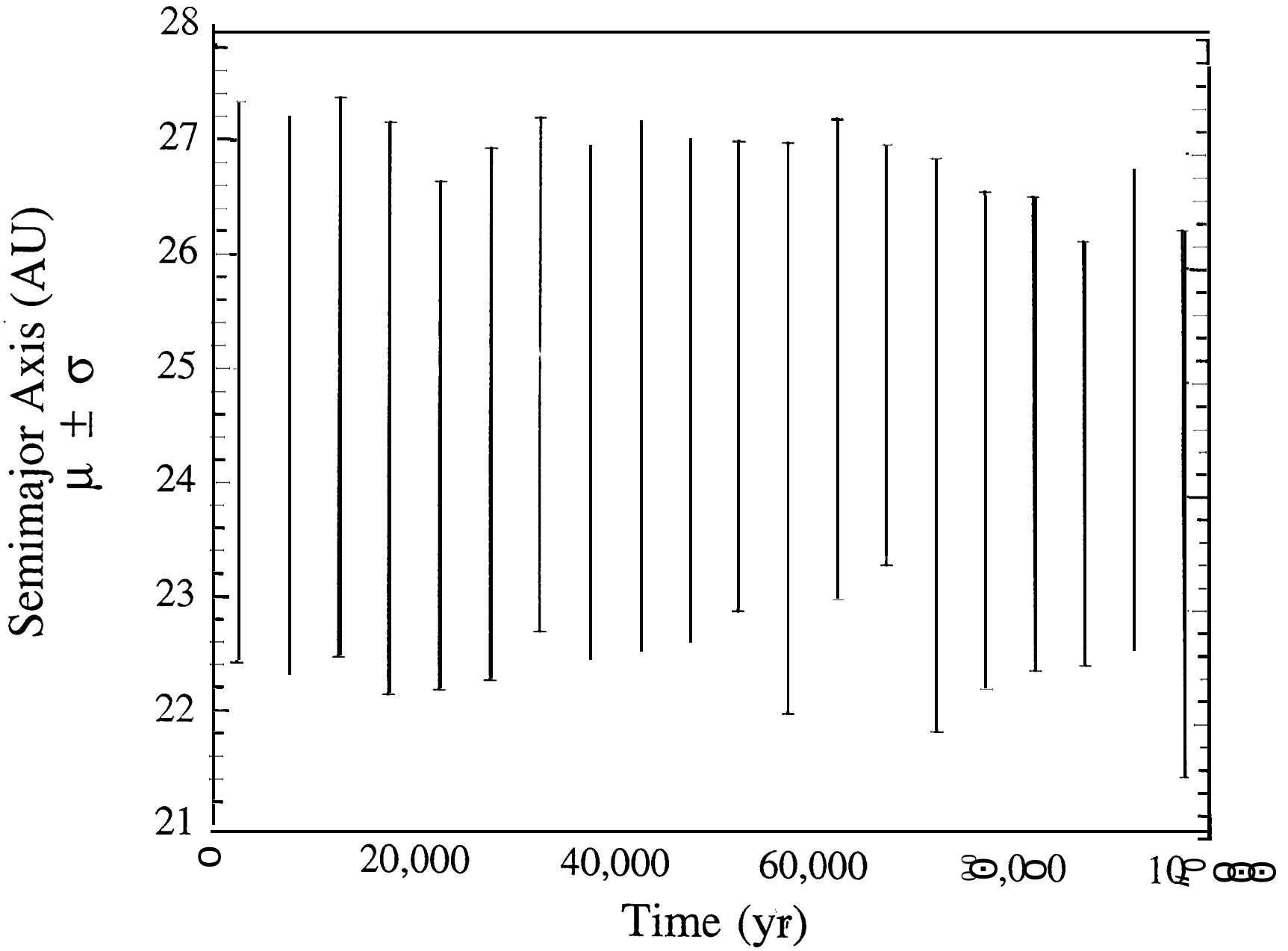
Semimajor Axis (AU)
μ ± σ
28
27
26
25
24
23
22
21
0
20,000
40,000
60,000
80,000
100,000
Time (yr)

Figure 16

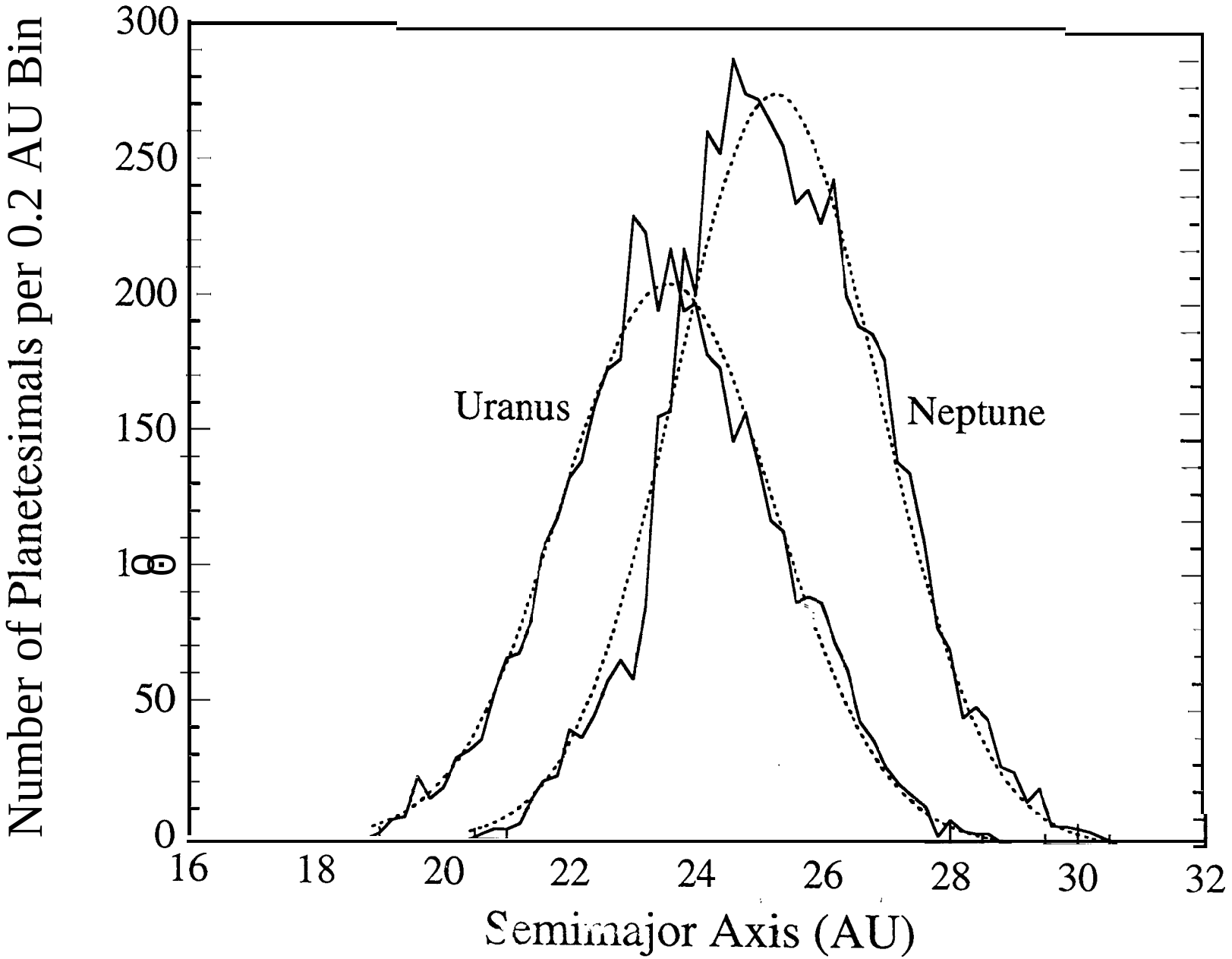
Number of Planetesimals per 0.2 AU Bin
300
250
200
150
100
50
0
16
18
20
22
24
26
28
30
32
Semimajor Axis (AU)
Uranus
Neptune

Figure 7

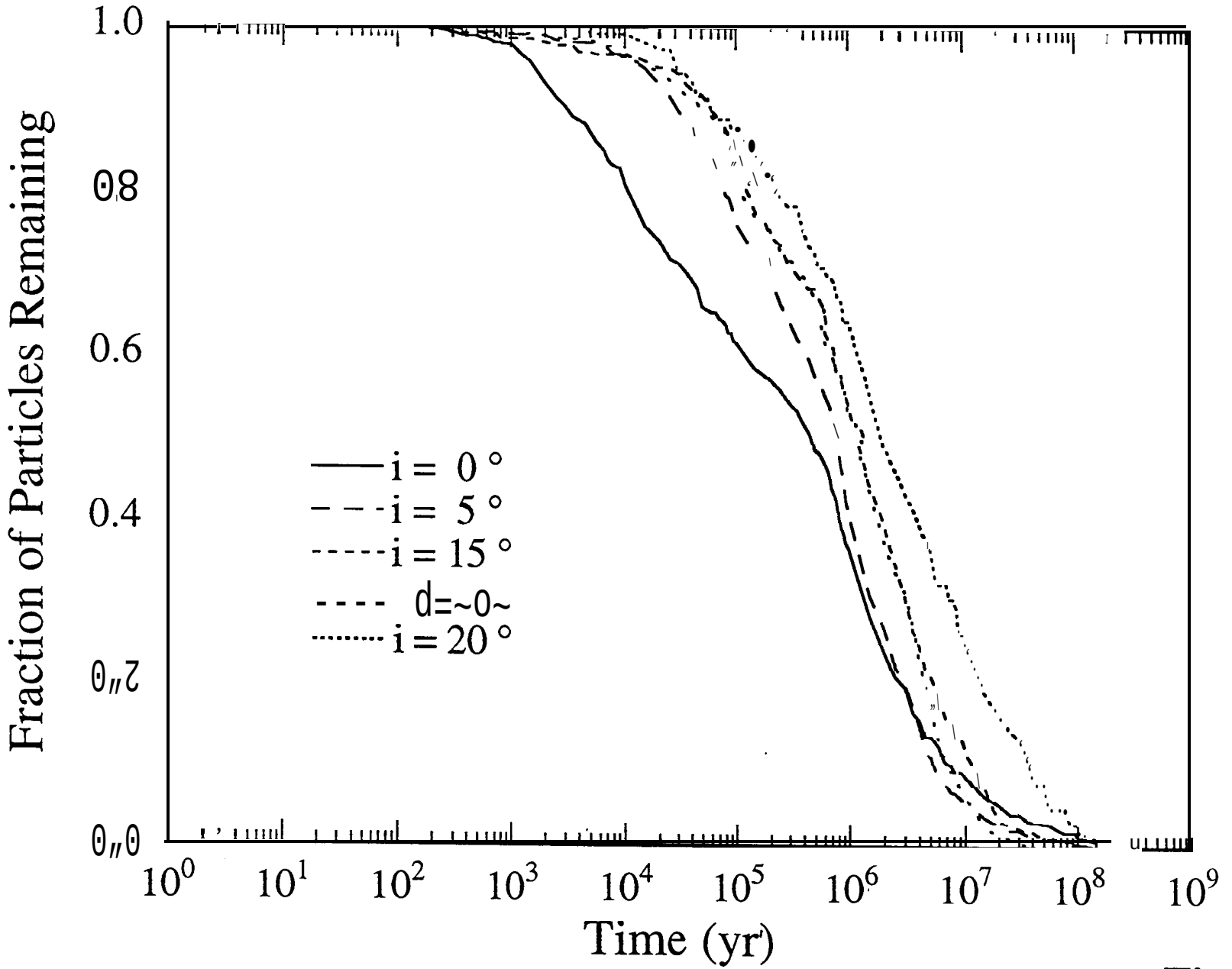
1.0
0.8
0.6
0.4
0.2
0.0
Fraction of Particles Remaining
i = 0 °
i = 5 °
i = 15 °
d=~0~
i = 20 °
10^0
10^1
10^2
10^3
10^4
10^5
10^6
10^7
10^8
10^9
Time (yr)

Figure 18

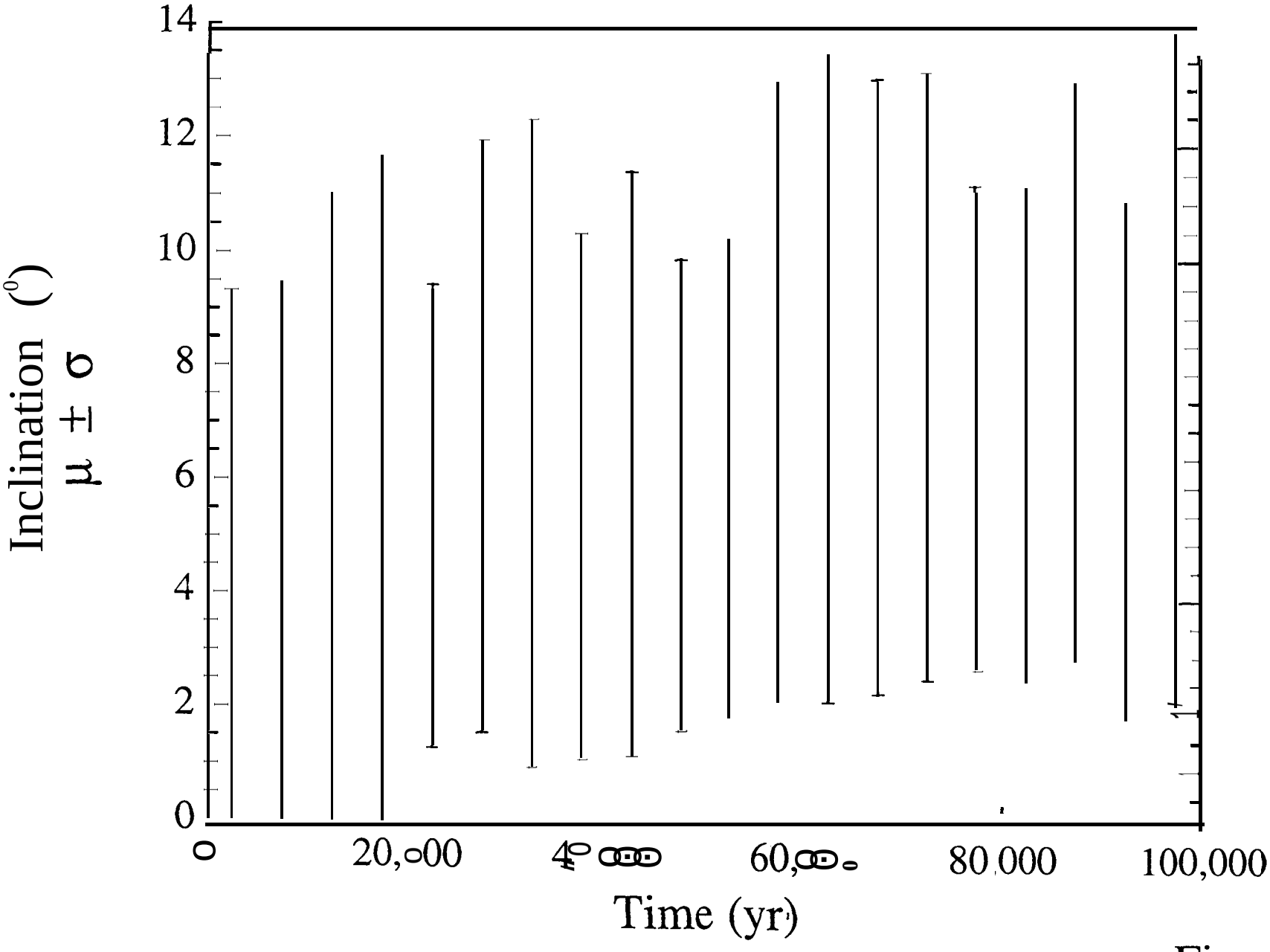
Inclination (°)
μ ± σ
14
12
10
8
6
4
2
0
0
20,000
40,000
60,000
80,000
100,000
Time (yr)

Figure 19

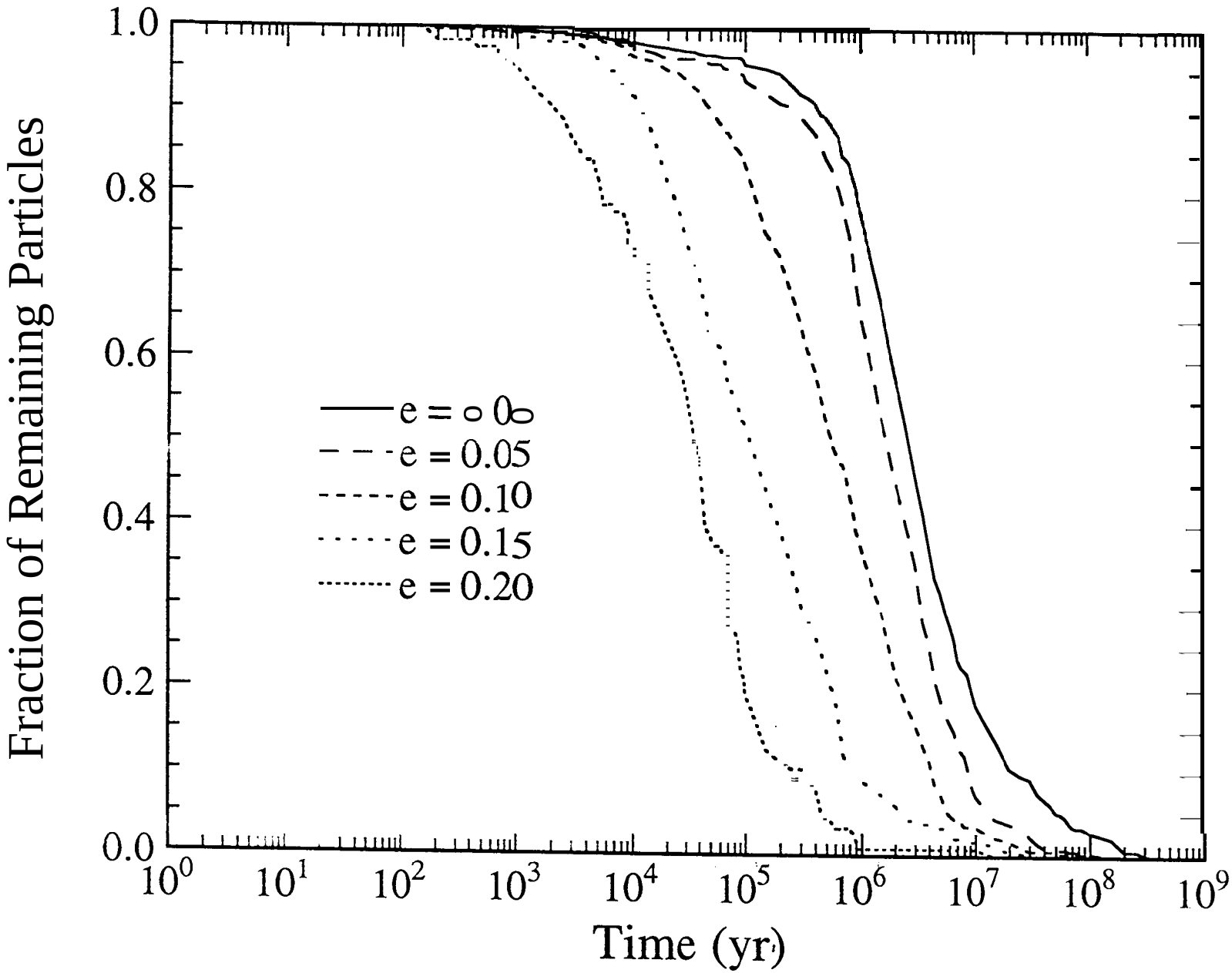
Fraction of Remaining Particles
1.0
0.8
0.6
0.4
0.2
0.0
e = 0.0
e = 0.05
e = 0.10
e = 0.15
e = 0.20
10^0
10^1
10^2
10^3
10^4
10^5
10^6
10^7
10^8
10^9
Time (yr)

Figure 20

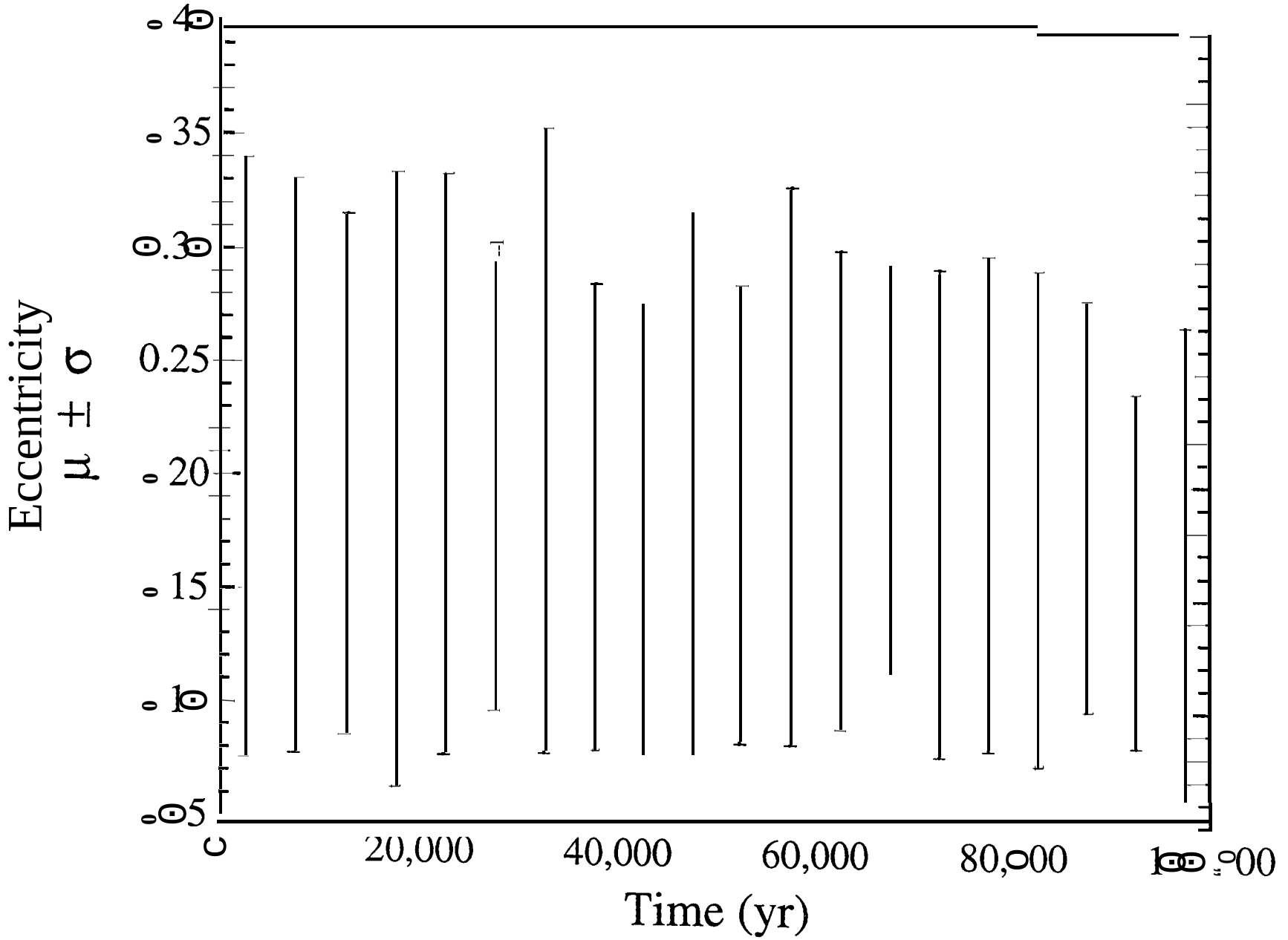
Eccentricity
μ ± σ
0.45
0.35
0.3
0.25
0.2
0.15
0.1
0.05
0
20,000
40,000
60,000
80,000
100,000
Time (yr)

Figure 21

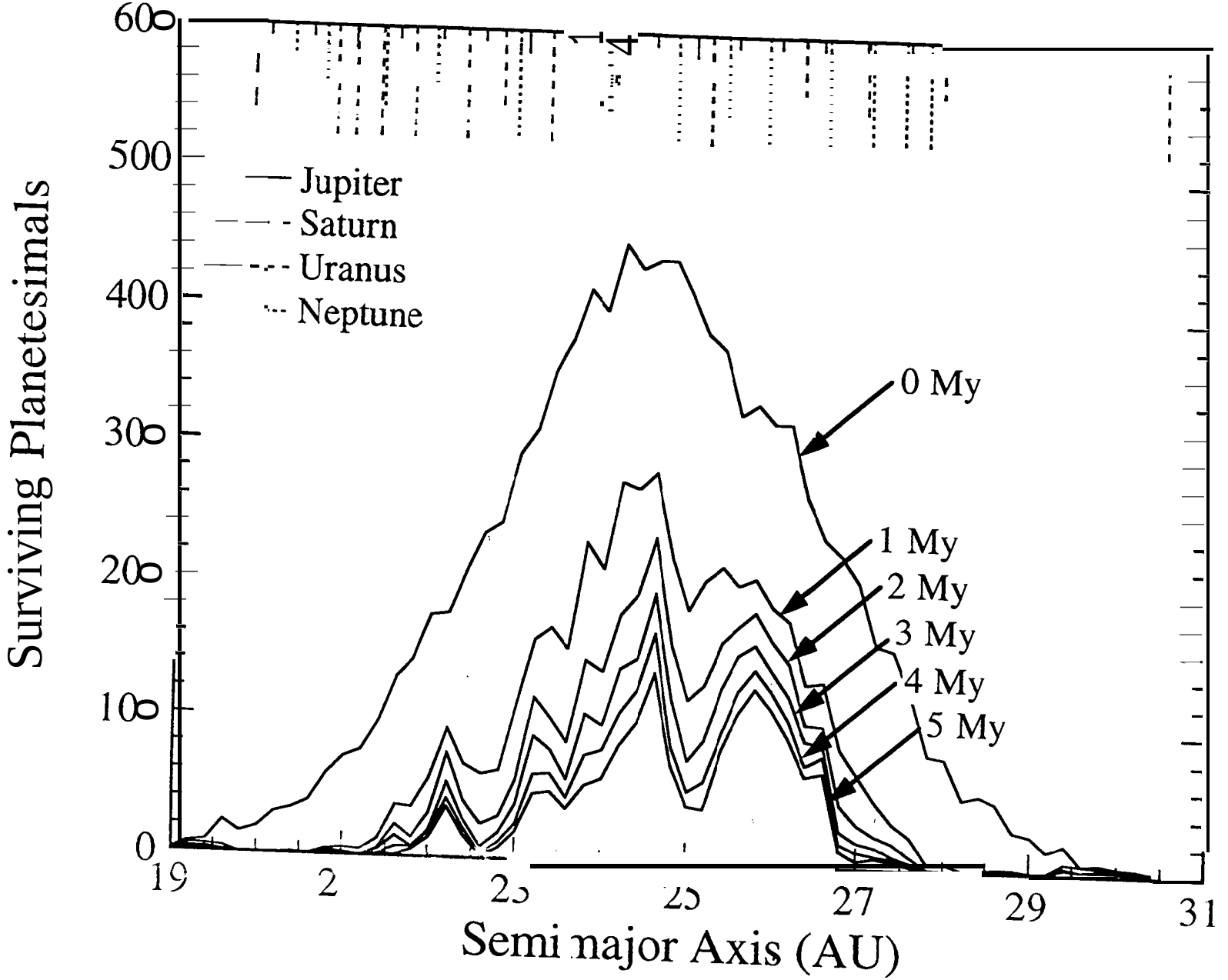
Surviving Planetesimals
600
500
400
300
200
100
0
Jupiter
Saturn
Uranus
Neptune
0 My
1 My
2 My
3 My
4 My
5 My
19
21
23
25
27
29
31
Semi major Axis (AU)

Figure 22

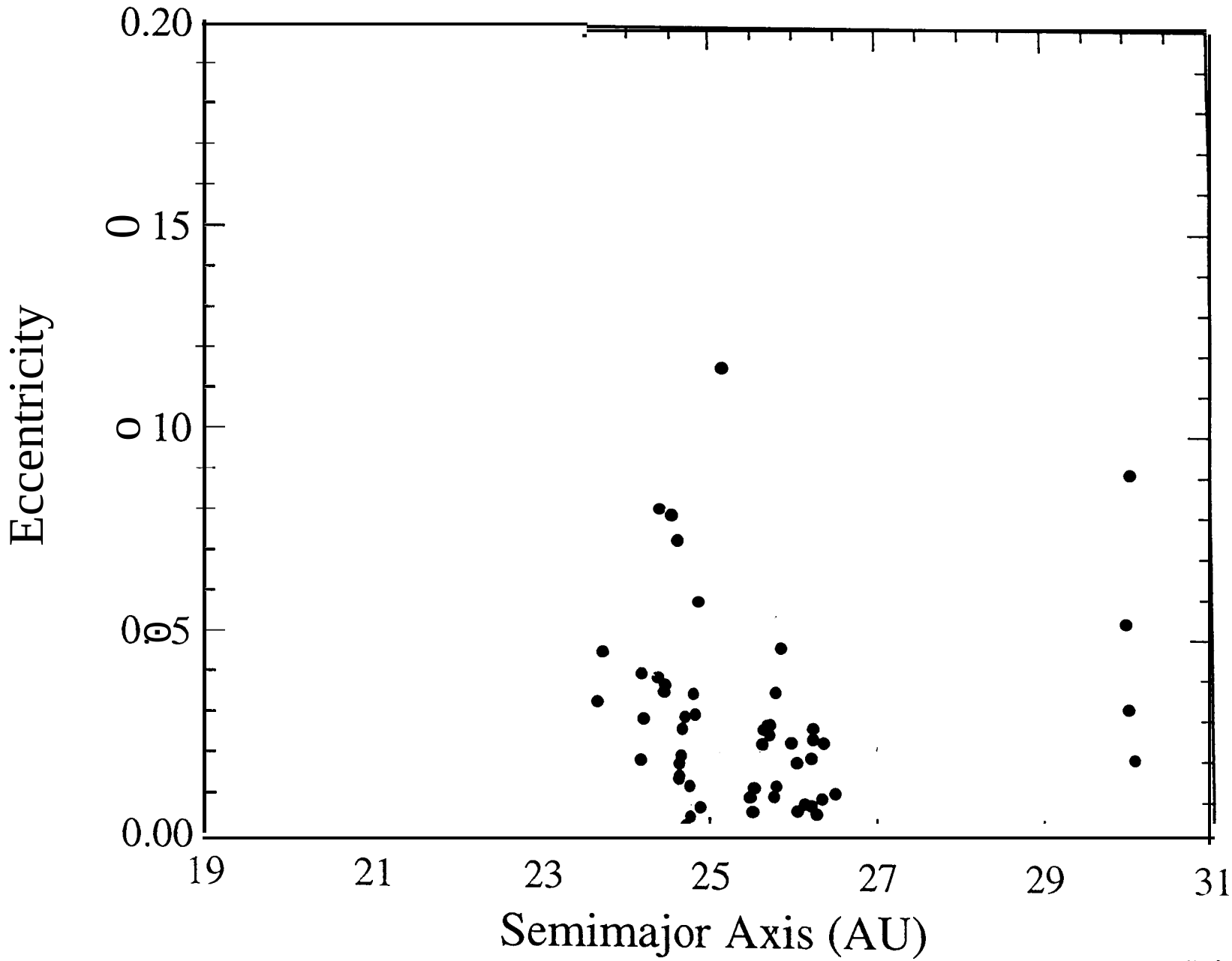
0.20
0 15
0 10
0@5
0.00
19
21
23
25
27
29
31
Eccentricity
Semimajor Axis (AU)

Figure 23